Scientific Spokesperson
S. Whitaker
Physics Department
Mass. Inst. of Tech.
Cambridge, MA
Phone (8) 835-7587

Proposal to Study Neutrino Interactions in a Beam Dump Experiment

D. Bogert, R. Brock, R. Fisk, T. Ohska, L. Stutte,
J. K. Walker, J. Wolson
Fermi National Accelerator Laboratory
Batavia, IL

R. Burg, W. Busza, J. Friedman, M. Goodman, H. Kendall,
T. Lyons, T. Mattison, L. Osborne, L. Rosenson,
M. Tartaglia, S. Whitaker, G.P. Yeh
Massachusetts Inst. of Technology
Cambridge, MA

M. Abolins, A. Cohen, J. Ernwein, D. Owen, J. Slate
Michigan State University
East Lansing, MI

F.E. Taylor
Northern Illinois University
Dekalb, IL

April 1980

72 pgs.

Contents

I. Introduction

In this proposal we describe the physics that the flash chamber-proportional tube calorimeter located in Lab C will be able to investigate using a beam dump facility. The unique feature of a beam dump facility is that it allows the production and interaction of prompt neutrinos to be studied. Furthermore, a search for new flavor neutrinos may be performed. When coupled to a large mass detector which has the capability of providing detailed information about event topology, such a facility has the potential of unveiling a rich domain of new phenomena.

In contrast to present high energy neutrino beams which consist mainly of muon neutrinos from the decay of pions and kaons, the neutrinos from a beam dump are expected to originate predominantly from the decays of charmed particles. Thus one expects in such a beam a strong component of electron neutrinos and possibly tau neutrinos in addition to the well-studied muon neutrinos. There is also the possibility of detecting some other unknown prompt neutrinos or new neutral particles which do not interact hadronically.

The Lab C detector is well suited to the study of such beams. It has sufficient mass to accumulate a statistically meaningful number of events for a number of interesting processes while having sufficient granularity and energy and angle measuring capability to allow the selection of events on the basis of topology. This greatly aids in the rejection of

background processes. The superb resolution of the detector will enable us to investigate the following physics topics:

1) Search for ν_τ. The detection of the ν_τ will be an important confirmation of the tau lepton family. Limits on the tau neutrino-electron neutrino mixing will be made.

2) A study of electron neutrino scattering. This will probe electro-weak interactions and will allow a new determination of $\sin^2\theta_w$.

3) Search for new phenomena. The very fine granularity of the flash chamber-proportional tube calorimeter will allow measurement of p_t imbalance which may characterize interesting phenomena. In addition, we will be able to study prompt neutrinos at large production angles where neutrinos from the decay of heavy particles will be enhanced.

II. Generation of Neutrinos in a Beam Dump

II.1 The Beam Dump Facility

The beam dump will consist of an assembly of tungsten plates and absorber material. It will be followed by a system of magnets and shielding to minimize the muon background in the detectors.[1] The angle of the proton beam onto the dump will be variable out to about 40 mrad. This will be extremely advantageous in the exploration of sources of prompt neutrinos.

The major prompt source of electron and muon neutrinos is expected to be the pair production of charmed D mesons and their subsequent decay. Thus we expect equal prompt yields of $(\bar{\nu})_e$ and $(\bar{\nu})_\mu$ neutrinos. This is however modified by a significant non-prompt source of muon neutrinos arising from π/K decay. Because of the large mass of the D relative to the π or K mesons, the ratio of non-prompt to prompt neutrino production is expected to diminish rapidly with increasing production angle.

There are good reasons to expect a ν_τ flux which originates from the decays of the as-yet-unobserved charmed F mesons. These are assumed to be pair produced in the dump and will contribute $(\bar{\nu})_\tau$'s both by direct F decay $F^\pm \to \tau^\pm + (\bar{\nu})_\tau$ and by the subsequent tau decay $\tau^\pm \to (\bar{\nu})_\tau + (\ell^\pm + (\bar{\nu})_\ell$ or hadrons). The fluxes of ν_τ and $\bar{\nu}_\tau$ depend on assumptions of the F meson production cross section and A dependence and on the F branching fractions.

An important aspect of the beam dump will be the capability to reconfigure the tungsten plates and vary the density of the target. This will vary the flux of neutrinos from nonprompt sources and will allow the prompt neutrino yield to be computed by extrapolating the measured yield versus inverse density to $1/\rho = 0$ -- infinite density. The beam dump density should be variable from $\rho = 1$ (full tungsten density) to $\rho = 1/3$. Roughly 1/4 of the proton exposure should be with $\rho = 1/3$ and roughly 3/4 with $\rho = 1$.

The extrapolation of muon neutrino signals to infinite density is expected to be different from that for tau neutrino signals. Muon neutrinos have several copious nonprompt sources such as π or K decay in addition to D decay as a prompt source. Tau neutrinos, on the other hand, are expected to come almost exclusively from F decay -- a prompt source. Hence the slope of the muon neutrino yield versus inverse density will be steeper than the corresponding slope of the yield of tau neutrino events. The dependence of the tau neutrino signal on beam dump density will constitute an important test for background due to muon neutrinos.

II.2 Calculated Neutrino Fluxes

S. Mori and J. K. Walker (TM - 953) have recently calculated the fluxes of ν_e and ν_τ type neutrinos from a beam dump facility. Figures 1 and 2 show the expected fluxes of ν_e and ν_τ neutrinos in Lab C from a dump located 190 meters upstream and struck by 1 TeV protons. The ν_e flux is assumed to arise from the decay of D mesons pair-produced in the dump. If D pairs were the only source of ν_e neutrinos, the flux of $\bar{\nu}_e$ would be equal to the flux of ν_e. The fluxes at zero degrees of ν_μ and $\bar{\nu}_\mu$ are expected to be about 50% larger than the ν_e flux due to the additional contributions from charged pions and kaons which decay before being absorbed in the dump.

II.3 Measurement of Fluxes

The fluxes of ν_μ and $\bar{\nu}_\mu$ will be monitored by the copious charged current deep inelastic reactions, where the sign of the outgoing muon will establish the nature of the incident neutrino. The sum of the fluxes of ν_e and $\bar{\nu}_e$ will be monitored by their charged current deep inelastic reactions in a restricted kinematic region of large x and moderate y where the angular separation of the electron and the hadron showers will allow their separate observation. The region in which this is possible will be established on the basis of results of tests of the detector in a calibration beam.

We expect to accumulate a total of $\sim 4 \times 10^5$ ν_e and $\bar{\nu}_e$ charged current inelastic semi-leptonic events for 2.5×10^{18} protons on the dump. In addition it will be possible to monitor the ν_e and $\bar{\nu}_e$ flux by observing the quasielastic reaction $\nu_e + n \rightarrow e^- + p$ and $\bar{\nu}_e + p \rightarrow e^+ + n$. The flash chamber detector is particularly well suited to detect the slow protons at large angle encountered in the neutrino-induced reaction; the proton is expected to be observable in roughly 1/4 of the events. In a run of 2.5×10^{18} protons incident on the dump we would accumulate approximately 1500 ν_e and 900 $\bar{\nu}_e$ quasielastic events.

III. Tau Neutrino Physics

The existence of the τ lepton, with a rest mass $m_\tau = 1.78$ GeV, is now well established on the basis of measurements made at the SPEAR and DORIS e^+e^- facilities. There are theoretical reasons to expect there to be a sequential neutrino, ν_τ, distinct from ν_μ and ν_e, associated with the τ. Results from the Columbia-BNL collaboration[2] show that

$$\frac{\nu_\mu + N \to \tau^- + X \to e^- + X}{\nu_\mu + N \to \mu^- + X} \leq 3 \times 10^{-3}$$

giving the coupling constant $g^2_{\tau\nu_\mu} < 0.025\ g^2_{\mu\nu_\mu}$. If $\nu_\mu = \nu_\tau$, this limit is incompatible with the observed τ-decay results. While experimental results rule out the possibility that $\nu_\tau = \nu_\mu$ there is no evidence to exclude the possibility that ν_e and ν_τ are identical or that there is substantial mixing between them. At the present time, no experiment has observed the production of a τ by a neutrino beam which could be interpreted as the interaction of a ν_τ. The direct observation of the ν_τ would be an important confirmation of the tau lepton family.

III.1 The Channel $\tau^{\pm} \rightarrow \mu^{\pm} + (\bar{\nu}_{\mu}) + \nu_{\tau}$

Recently, Albright, Shrock, and Smith[3] have proposed a test which can be used to make such an observation in a beam dump experiment. This test involves the detection of the charged current reaction

$$(\bar{\nu}_{\tau}) + N \rightarrow \tau^{\pm} + \underline{\bar{X}} \text{ with } \tau^{\pm} \rightarrow \mu^{\pm} + (\bar{\nu}_{\tau}) + (\bar{\nu}_{\mu})$$

which can serve as a reliable signal of a ν_{τ} interaction. The two neutrinos carry off substantial momentum which results in a sizable imbalance in the momentum measured transverse to the neutrino beam direction. This momentum imbalance serves as an important signature of this reaction. The charge of the muon indicates whether the interaction was induced by a neutrino or anti-neutrino. Figure 3 gives a diagram of the reaction and depicts an event projected onto the plane perpendicular to the beam direction to illustrate the transverse momentum imbalance.

The ν_{τ} and $\bar{\nu}_{\tau}$-induced events in the Lab C detector will have the following special features which will help to separate these events from background events:

1. P_t imbalance, shown in Fig. 4b.
2. The distribution of azimuthal opening angles between the hadron shower and the missing P_t will be peaked at 180° as shown in Fig. 4a.
3. The X_{vis} distribution determined by the visible energy and momentum transfer is sharply peaked toward 0, as shown in Fig. 4c.
4. The y_{vis} distributions are strongly shifted to high y as shown in Fig. 4d.

Here x_{vis} and y_{vis} are the scaling variables calculated using the observed quantities:

$$x_{vis} = \frac{2(E_H + E_\mu)\, E_\mu \sin^2\frac{\theta_\mu}{2}}{M_N\, E_H}$$

$$y_{vis} = \frac{E_H}{E_H + E_\mu}$$

Using the estimated ν_τ fluxes given in Fig. 2, we calculate that 3.8×10^4 $\tau^\pm$ leptons will be produced in 150 fiducial tons of the 330 ton Lab. C detector for a total of 2.5×10^{18} protons incident on the dump. (Due to the inherent uncertainty in the ν_τ flux we have ignored mass effects and simply taken $\sigma_{\nu_\tau}^{cc} = \sigma_{\nu_\mu}^{cc}$. Averaged over the energy-weighted ν_τ spectrum, this is $\sim$ 20% too high.) Under standard Tevatron running conditions, 2.5×10^{18} protons correspond to about one half a year of running at unit efficiency. Using the measured branching ratio of 17%, one expects to observe about 6330 $\tau \rightarrow \mu + \nu + \bar{\nu}$ events.

If we cut these events with P_t missing > 2 GeV, where P_t missing $= |P_{t\mu} + P_{t\ had}|$, we reduce the signal by a factor of 2. The major background to this signal is mismeasured $\nu_\mu + \bar{\nu}_\mu$ charged-current events. With the resolutions inherent in our detector, described in Appendix A, P_t missing can be measured with an error $\sigma_{P_t\text{missing}} \sim 0.7$ GeV/c, which requires the measurement on the background events to have an error of 3 standard deviations in order to satisfy the cut. In the expectation that the resolution tails will be higher than

those given by a gaussian, we make a more conservative estimate by assuming that only a reduction in the background to the $\geq 2\sigma$ level is possible. To separate the signal from this background one has to examine the distribution of the azimuthal angle between $P_{t\ missing}$ and the transverse momentum of the hadron shower. This distribution should be flat for the background events whereas it should be strongly peaked around $\Delta\phi_{mH} = 180^{o}$ for the signal. Figure 5 shows the expected distributions for both the signal and background. The experimental resolution in ϕ is expected to be $\lesssim 1/2$ of the peak full width. The background yield beneath the signal "peak" is expected to be about 4.5 K events.

A further reduction in background could be obtained by making a cut on x_{vis}. For example, a cut on $x_{vis} \leq .2$ would reduce the signal by only about 10%, but would reduce the background by about 50%. It is clear in Fig. 5 that the background beneath the signal can be reasonably well estimated from the yields for $\Delta\phi_{mH} \lesssim 135^{o}$. In all likelihood the distribution of background for all $\Delta\phi_{mH}$ will have been determined from the prior use of this detector to measure ν_{μ} and $\bar{\nu}_{\mu}$ charged-current events. These considerations lead us to believe that we will be able to find a τ signal if it exists at this level. Table I summarizes the results we expect in this channel.

TABLE I

YIELDS FOR $\tau \rightarrow \mu \bar{\nu}_\mu \nu_\tau + \tau^+ \rightarrow \mu^+ \nu_\mu \bar{\nu}_\tau$

The number of taus produced in 150 ton fiducial volume from 2.5×10^{18} protons.	$3.75\ 10^4$
The number of the above which decay $\tau \rightarrow \mu\nu\nu$	6330
The number of the above with $p_{tm} > 2$ GeV	3170
Estimated background with $p_{tm} > 2$ GeV and $135^\circ < \phi_{mh} < 180^\circ$	4500
The number of the above with $p_{tm} > 2$ GeV and $x_{vis} < .2$	2800
Estimated background with $p_{tm} > 2$ Gev and $135^\circ < \Delta\phi_{mh}\ 180^\circ$ and $x_{vis} < .2$	2300

Other possible sources of background have been shown by Albright et al.[3] to be of negligible consequence. Ordinary neutral current events with a π or K decaying into a muon can be eliminated with a suitable muon energy and P_t cut; neutral current-induced charmed pair production followed by one semi-leptonic decay has a cross section times branching ratio that is negligibly small; ν_μ-induced single charm production with the decay of the charmed particle into the electron mode and the electron shower misidentified as part of the hadron shower is completely eliminated by the $P_{tmissing}$ and $\Delta\phi_{mH}$ cuts; and $(\bar{\nu})_e$-induced single charm production with the decay of the charmed particle into the muon mode, again with the electron shower misidentified as part of the hadron shower, also is removed by the $P_{tmissing}$ cut.

III.2 The channel $\tau^\pm \to \pi^\pm (\bar{\nu})_\tau$

In addition to the $\tau \to \mu + \nu + \bar{\nu}$, the decay channel $\tau \to \pi + \nu$, depicted in Fig. 6, may be detected in our calorimeter. The ability to detect an additional channel would increase our confidence that the observed signal of muon events with missing P_t in fact arose from τ decays. The interpretation of the data as being due to τ production would require that the two channels be observed in the ratio of the branching fractions of the τ as measured at DORIS and SPEAR.

The experimental signature of the π channel is the observation of a single particle with energy > 15 GeV at a large angle with respect to the direction of the primary hadron shower, this track being observed to penetrate $\gtrsim$ 5 radiation lengths without interacting and then to interact producing a hadronic shower. We expect the π channel to be discernable in our detector because the τ's are primarily produced at large P_t with respect to the neutrino direction. For example, for τ's produced by 100 GeV neutrinos (approximately the mean τ production energy), the mean P_t is 2.5 GeV. Thus, requiring that the hadron shower produced in association with the τ has a P_t > 1.5 GeV insures a large opening angle between the π and the hadronic shower. With this cut we lose only about 22% of the events. It is not likely that a high energy π (E>15 GeV) from the hadronic shower would be within a P_t of about 1 GeV with respect to the τ direction since the τ momentum vector tends to be about 10^{o} away from the hadronic shower direction for the above P_t cut and the hadron shower has a mean spread of P_t of about .3 GeV/c with respect to its mean direction.

Our capability to observe this channel hinges on the important question of whether the width of the hadronic shower is sufficiently great to obscure this type of event. The measurements of Friend et al.[4] give the result that the FWHM of the energy deposition of a shower induced by a 10 GeV pion is within ± 65 mrad and that the width is approximately independent of energy. Figure 7 shows a 100 GeV pion-induced

shower as observed in our test calorimeter; superposed on that figure are lines indicating the $\sim$5 radiation length and $\sim$10 degree cuts which we would apply to select candidates for this channel. Calibration of our detector with a hadron beam in June 1980, will provide the data required to evaluate the optimum cuts to maximise the signal to background for observation of the ν_τ in this way.

The major physics background to the $\tau \rightarrow \pi$ signal arises from a neutral current event in which one of the hadrons in the shower has a large P_t with respect to the shower axis. Estimates based on the measurements and fits of inclusive spectra of Taylor et al.[5] and measurements of the P_t distributions of leptoproduced hadrons[6] indicate that this background creates a contamination of less than 20 events. These estimates lead us to believe that this channel will also be measurable in a beam dump exposure. Table II summarizes the results we expect in this channel.

TABLE II

Yields for $\tau \rightarrow \pi\nu$

The number of taus produced in 150 ton fiducial volume from 2.5×10^{18} protons	3.75×10^4
The number of the above which decay $\tau \rightarrow \pi\nu$	2900
The number with cut $p_{tH} > 1.5$ GeV	2300
The number with cut $P_{tH} > 1.5$ GeV and $p_\pi > 15$ GeV and $\theta_{\pi H} > 10^o$	1000
The number with all cuts which will not interact in .7 absorbtion lengths	500
Estimated Background from high-p_t-hadron neutral current events	20

III.3 Limit on Neutrino Mixing

Two questions can be addressed when the tau neutrino signal is observed: 1) Is the ν_τ identical to ν_e? 2) Is there some mixing between the ν_τ and the ν_e? A large number of tau events, comparable to the number of events of the type $(\bar{\nu}_e) + N \rightarrow e^{\pm} X$, would correspond to the two neutrino types being identical or having a nearly maximal mixing. A small number of tau events, of the order of 5% of the number of $(\bar{\nu}_e)$ - induced events, would correspond to a maximum mass difference of 10 eV between the two neutrino mass states for a mixing angle of 45°. When the $F\bar{F}$ production cross section and the $F \rightarrow \tau \nu_\tau$ branching ratios are ultimately determined, one will be able to put a much more stringent limit on the combined effects of mixing and mass difference.

While there are good limits for ν_e and ν_μ mixing, obtained from high energy neutrino scattering measurements, there are no reliable limits on ν_e neutrino mixing with any other type of neutrino, such as that which would be associated with the tau lepton. In fact, Reines et al.[7] have recently reported evidence at the 3σ level for $\bar{\nu}_e$ mixing with an unidentified neutrino. There are also some very interesting results from the most recent CERN beam dump experiment, where several different groups have observed the ratio $(\nu_e+\bar{\nu}_e)_{prompt}/(\nu_\mu + \bar{\nu}_\mu)_{prompt} \approx 0.5$, deviating from unity by several σ. The CHARM collaboration has also reported the observation of an excess of neutral current events at low energy. It has been suggested by De Rujula et al.[8] that these results may be interpreted as indications for $\nu_e \leftrightarrow \nu_\tau$ oscillations.

Neutrino mixing increases with the parameter $\frac{m_1^2-m_2^2}{2E_\nu}.x$ for small values of the parameter, where m_1 and m_2 are the eigenvalues of the mass matrix, x is the distance of the detector from the dump, and E_ν is the energy. It is clear that mixing would produce a higher fraction of low energy tau events than would the hypothetical production process involving F mesons. The energy spectrum of the observed tau events would thus provide information that could help disentangle the production mechanism. We hope to elucidate this question with high statistics and good resolution and pattern recognition at the low energies where these effects occur.

IV. Electron Neutrino Physics

IV.1

The production of neutrinos in a dump is expected to result in approximately equal fluxes of ν_μ, $\bar{\nu}_\mu$, ν_e, and $\bar{\nu}_e$. As a consequence, this type of experiment provides an excellent and unique opportunity to study the interactions of high energy electron neutrinos in both purely leptonic and semi-leptonic processes. Here, we report on the capability of the Lab C detector to study $\overset{(-)}{\nu}_e + e^- \rightarrow \overset{(-)}{\nu}_e + e^-$ in a beam dump experiment.

Unlike other neutral current processes, the scattering of ν_e or $\bar{\nu}_e$ from electrons involves both charged and neutral-current amplitudes and thus should be sensitive to their interference. All surviving gauge models predict a negative sign for this interference. Thus, while such a measurement cannot distinguish between such models unless it is sufficiently accurate, a 25% measurement can determine the sign of interference[9] and determine whether the popular models are consistent with this determination. A 10% measurement of the total $\nu_e + e$ cross section could determine $\sin^2\theta_w$ to $\pm$ .03. Such a measurement could decisively exclude the (V-A) model, since the (V-A) cross section is a factor of 1.7 greater than the Weinberg-Salam prediction for a Weinberg angle of $\sin^2\theta_w \sim .25$.

One will not be able to determine the identity of the incident neutrino in a ν-e elastic scattering, and as ν_e, $\bar{\nu}_e$, ν_μ. and $\bar{\nu}_\mu$ are expected to be present in about equal number, one will measure the sum of all four elastic cross sections. On the basis of the Weinberg-Salam model and $\sin^2\theta_w = .25$, one expects the event ratio to be 7:3:1:1 for incident ν_e, $\bar{\nu}_e$, ν_μ, and $\bar{\nu}_\mu$ respectively. The elastic $\nu_\mu e$ and $\bar{\nu}_\mu e$ events will comprise about 15% of the total. There is already some good information about the $\nu_\mu e$ cross section[10], and we expect that before a Tevatron beam dump program this cross section and the $\bar{\nu}_\mu e$ cross section will be well known from 400 GeV wide band measurements to be made with the Lab C detector and from the work of other groups. With the subtraction of the $\nu_\mu e$ and $\bar{\nu}_\mu e$ yields we thus will be able to measure the sum of ν_e e and $\bar{\nu}_e$ e elastic events. This measurement can be made during the running devoted to the search for the tau neutrino. The use of 10 pings (of about 2 ms each) per spill will reduce detector dead time from semi-leptonic events sufficiently so that no special fast electronics trigger will be required to observe the elastic $(\bar{\nu}_e)$ events with high efficiency. This point is discussed in more detail in Appendix B. For a run of 2.5×10^{18} protons incident on the dump we would expect to observe 250 ν_e e and $\bar{\nu}_e$ e elastic events.

The ultimate success of this measurement will depend on how well we remove the backgrounds from the yields. The major sources of background are the following:

(a) Inverse beta-decay of the neutron and proton $\nu_e n \rightarrow e^- p$ and $\bar{\nu}_e\ p \rightarrow e^+ n$

(b) Single π^o production by the neutral current neutrino interaction causing an electro-magnetic shower and thus simulating an electron.

(c) Very low x and y inelastic semi-leptonic ν_e and $\bar{\nu}_e$ reactions in which the low energy hadronic shower is obscured by the electron shower

Estimates of Backgrounds

The backgrounds from the processes $\nu_e + n \rightarrow p + e^-$ and $\bar{\nu}_e + p \rightarrow n + e^+$ have been calculated using the expression

$$\frac{d\sigma}{dQ^2} = \frac{G^2}{\pi}\left[\frac{F_A^{\,2} + F_V^{\,2}}{2}\right]$$

where

$$\frac{F_A}{1.23} = F_V = \frac{1}{\left[1 + \frac{Q^2}{.84}\right]^2}$$

It has been shown [11] that when these processes take place on bound nucleons there will be significant suppression of the yields at low momentum transfers due to Pauli exclusion. This effect has been included in the background calculations as a factor $R(\vec{Q}^2)$ times the cross section,

$$R(\vec{Q}) = \begin{cases} \frac{3}{2}(\frac{\vec{Q}}{2p_F}) - \frac{1}{2}(\frac{\vec{Q}}{2p_F})^3 & \text{for } \vec{Q} < 2p_F \\ 1 & \text{for } \vec{Q} > 2p_F \end{cases}$$

where

$$|\vec{Q}| = \sqrt{Q^2 (1 + \frac{Q^2}{4M^2})} \quad \text{and } p_F = 0.266 \text{ MeV/c.}$$

This low Q^2 suppression reduces the background substantially beneath the elastic ν_e, e peak. Electrons from elastic ν_e,e scattering are peaked in a forward cone of angle $\theta_e \tilde{=} \sqrt{\frac{2m_e}{E_\nu}}$ where E_ν is the energy of the incident neutrino. They are therefore confined to smalltransverse momenta $P_t \lesssim 200$ MeV/c. Electrons from the inverse beta-decay process have a much broader P_t distribution with a mean $P_t \gtrsim 500$ MeV. For a cut of $P_t \lesssim 200$ MeV which contains essentially the entire electron peak the background yield from the above processes is about 50% of the yield from the elastic peak. The inclusion of smearing effects due to experimental resolutions increases the ratio of background to elastic peak yield by about a factor of 4 within this cut. This relatively flat background can be subtracted from the yield in the region of the elastic peak by observing the inverse beta-decay rates at higher P_t and using the predicted curve to extrapolate to small P_t.

A second source of background arises from ν_e and $(\bar{\nu})_e$ charged current hadronic events at very low P_t in which the hadronic shower is lost within the electron shower. Because of the fine granularity of the detector and the much larger angular spread of hadronic showers we should be able to identify a hadronic shower of $E_h > 1$ GeV at the vertex of the event. Since the ν_e e elastic events occur at $P_t \lesssim 200$ MeV and the hadronic events have a mean P_t in the neighborhood of 2.5 GeV, the P_t cut alone substantially reduces this background. The hadronic events which escape the cuts of $E_h \lesssim 1$ GeV and $P_t \lesssim 200$ MeV, and thus can be confused with elastic ν_e e events cause about a 12% background under the elastic ν_e e peak, including resolution smearing.

A third source of background can arise from $(\bar{\nu})_\ell + N \rightarrow (\bar{\nu})_\ell + N\pi^o$. Present data on this reaction indicate that the $(N\pi^o)$ system is dominantly (1236). One can express the energy of the Δ as:

$$E_\Delta = \frac{M^2 + M_N{}^2 + Q^2}{2M_n}$$

so that the kinetic energy is roughly the same as that of the proton in inverse beta-decay. If one considers the worst case, i.e., the π^o takes away the maximum possible energy, $E_{\pi^o} \gtrsim E_\Delta - M_N$, then

$$E_{\pi^o} = \frac{M_\Delta{}^2 - M_N{}^2 + Q^2}{2M_N}$$

With the assumption that this reaction is strongly damped by hadronic form factors similar to the corresponding charged current single-pion reactions[12], an estimate has been made of this background. In this model, the ratio of rates for elastic $(\bar{\nu})_e$,e reactions and for $\nu N \rightarrow \nu N\pi^o$ processes is 1:33. Table III gives predictions of event signal to background ratios for various cuts. These results indicate that this background is not expected to cause any serious problems. If we are able to achieve a 15% measurement for the sum of the ν_e and $\bar{\nu}_e$ cross sections we will be able to determine $\sin^2\theta_w$ to $\pm.04$ for values of $\sin^2\theta_w$ in the neighborhood of 0.25.

TABLE III

Cut	$\frac{(\nu_e e \to \nu_e e) + (\bar{\nu}_e e \to \bar{\nu}_e e)}{\nu_\ell N \to \nu_\ell N \pi^o}$
None	1/33
$E_\gamma > 1$ GeV	5/1
and $E_\gamma > 1$ GeV $p_t^\gamma < 0.2$ GeV	75/1
$E_\gamma > 1$ GeV $p_{t\gamma} < 0.2$ GeV $\theta_\gamma < 100$ mrad	150/1

IV.2 Tests of ν_e - ν_μ universality

As discussed in Section II.2, the flux of ν_e and $\bar{\nu}_e$ will be monitored by the deep inelastic charged current reactions and by the quasielastic reactions. The quasielastic scattering is a low Q^2 process, while the deep inelastic scattering is a large Q^2 process. The comparison of these processes for muon neutrinos with those for electron neutrinos will allow ν_e - ν_μ universality to be tested at large Q^2. Similarly, the study of the x and y distributions for the $(\bar{\nu})_e$ deep inelastic reactions will have bearing on the issue of ν_e - ν_μ universality. As mentioned before, the kinematic region in which we will be able to make this measurement will be established on the basis of results of tests of the detector in a calibration beam.

V. New Phenomena

So far we have assumed that all events detected in Lab C from a beam dump facility would be due to neutrinos arising from the decay of charmed particles. While this expectation is reasonable, it is not necessarily correct, and it remains to be verified experimentally. Once x and p_t distributions for the hadronic production of charm are measured in a hadron experiment, the energy and angular spectra of prompt neutrinos could be studied to see if other sources were present. Other processes which are more speculative might contribute. These include:

1) Other hadronic sources of prompt neutrinos such as semileptonic decays of hadrons with new quantum numbers. Since these particles would be heavy and have more available p_t for the produced neutrino, this could lead to a dramatic increase in high energy neutrinos away from the center of the detector.

2) Other new particles, such as heavy leptons which decay weakly with the emission of a prompt neutrino.

3) Long lived neutral leptons, axions, higglets, etc. which would traverse the dump and would provide an apparent excess of neutral current events. The best limits on the possible existence of some of these particles come from the results of previous beam dump experiments. The proposed experiment should reduce these limits by at least two orders of magnitude. The above particles could interact in our detector or alternatively could decay in the 200' drift space between the 15' bubble chamber and Lab C. To trigger on such decays a proportional chamber will be located at the front of our detector to identify at least two particles in fast coincidence. When such a coincidence occurs the normal front veto counter signal will be aborted and a trigger will be allowed.

In the exploration of the processes mentioned above it will be extremely advantageous to be able to control the angle of the proton beam on to the dump. In this way the normal prompt $\overset{(-)}{\nu}_e$, $\overset{(-)}{\nu}_\mu$ and $\overset{(-)}{\nu}_\tau$ neutrinos from charm can be suppressed relative to the new source. For this reason we request runs at incident proton angles of 15 mrad and 40 mrad in addition to the main run which will be at zero degrees.

VI. SUMMARY

The combination of a beam dump facility and the fine grained calorimeter in Lab C will permit the study of several exciting new areas in high energy physics. These will include the search for the tau neutrino, electron neutrino elastic and inelastic reactions, electron neutrino-tau neutrino mixing, and prompt neutrino production at large angles. For 2.5×10^{18} protons on the dump we expect to accumualte approximately 8×10^{5} neutrino interactions. These high statistics coupled with the detailed information provided by the detector will enable us to make important additions to our knowledge of weak interactions.

VII. Requests

We request the following runs at 1 TeV:

Proton Angle of Incidence on Beam Dump	Number of Protons
0^{o}	2.5×10^{18}
15 mr	5×10^{17}
40 mr	5×10^{17}

In Appendix C we discuss the possibility of operation at 400 GeV. We conclude that the physics potential of this study with the E-594 detector and 400 GeV protons on the dump is sufficient to justify immediate construction of the dump and operation at 400 GeV if 1 TeV is not available at that time. The above requests for angles and beam integrated beam would become:

0^{o}	5×10^{18}
15 mr	1×10^{18}
40 mr	1×10^{18}

References and Notes

1. The design of the beam dump and the active shielding will be specified in a forthcoming TM.
2. A.M. Cnops et al., Phys. Rev. Lett. 40, 144 (1978).
3. C.H. Albright et al., Phys. Lett. 84B, 123 (1979); Phys. Rev. D20, 2177 (1979).
4. B. Friend et al., Nucl.Instrum. Methods 136, 505 (1976).
5. F. E. Taylor et al., Phys. Rev. D14, 1217 (1976).
6. W. A. Loomis et al., Phys. Rev. D19, 2543 (1979).
   J. F. Martin et al., Phys. Lett. 65B, 483 (1976).
7. F. Reines et al., U.C. Irvine preprint, April 1980.
8. A. DeRujula et al., CERN preprint TH.2788, November 1979.
9. B. Kayser et al., Phys. Rev. D20, 87 (1979).
10. R. Heisterberg et al., Phys. Rev. Lett. 44, 635 (1980); C. Baltay, Proceedings of the Nineteenth International Conference on High Energy Physics, Tokyo, August 1978.
11. J.S. Bell and C.H. Llewellyn Smith, Nucl. Phys. B28, 317 (1971).
12. L. M. Sehgal, Phenomenology of Neutrino Reactions, ANL/HEP/PR75-45 (1975).

Figure Captions

1. Estimated ν_e flux from the dump at various distances.
2. Estimated ν_τ flux from the dump at various distances.
3. a. The process $\overset{(-)}{\nu}_\tau + N \rightarrow \tau^\pm +$ hadrons
   $\hookrightarrow \mu^\pm \; \overset{(-)}{\nu}_\mu \; \overset{(-)}{\nu}_\tau$

   b. Transverse momenta for the above process
4. Distributions for the process shown in figure 3:
   a. azimuthal opening angle $\Delta\phi_{mh}$
   b. missing transverse momentum $P_{t\ missing}$
   c. X_{vis}
   d. Y_{vis}

   The solid (dashed) curves are for ν_τ ($\bar{\nu}_\tau$) reactions.
5. Comparison of the $\Delta\phi_{mh}$ distributions from ν_τ events and from background.
6. The process $\overset{(-)}{\nu}_\tau + N \rightarrow \tau^\pm +$ hadrons
   $\hookrightarrow \pi^\pm \; \overset{(-)}{\nu}_\tau$
7. A 100 GeV pion-induced shower observed in a test calorimeter. Cuts relevant to the $\tau \rightarrow \pi$ channel are shown.

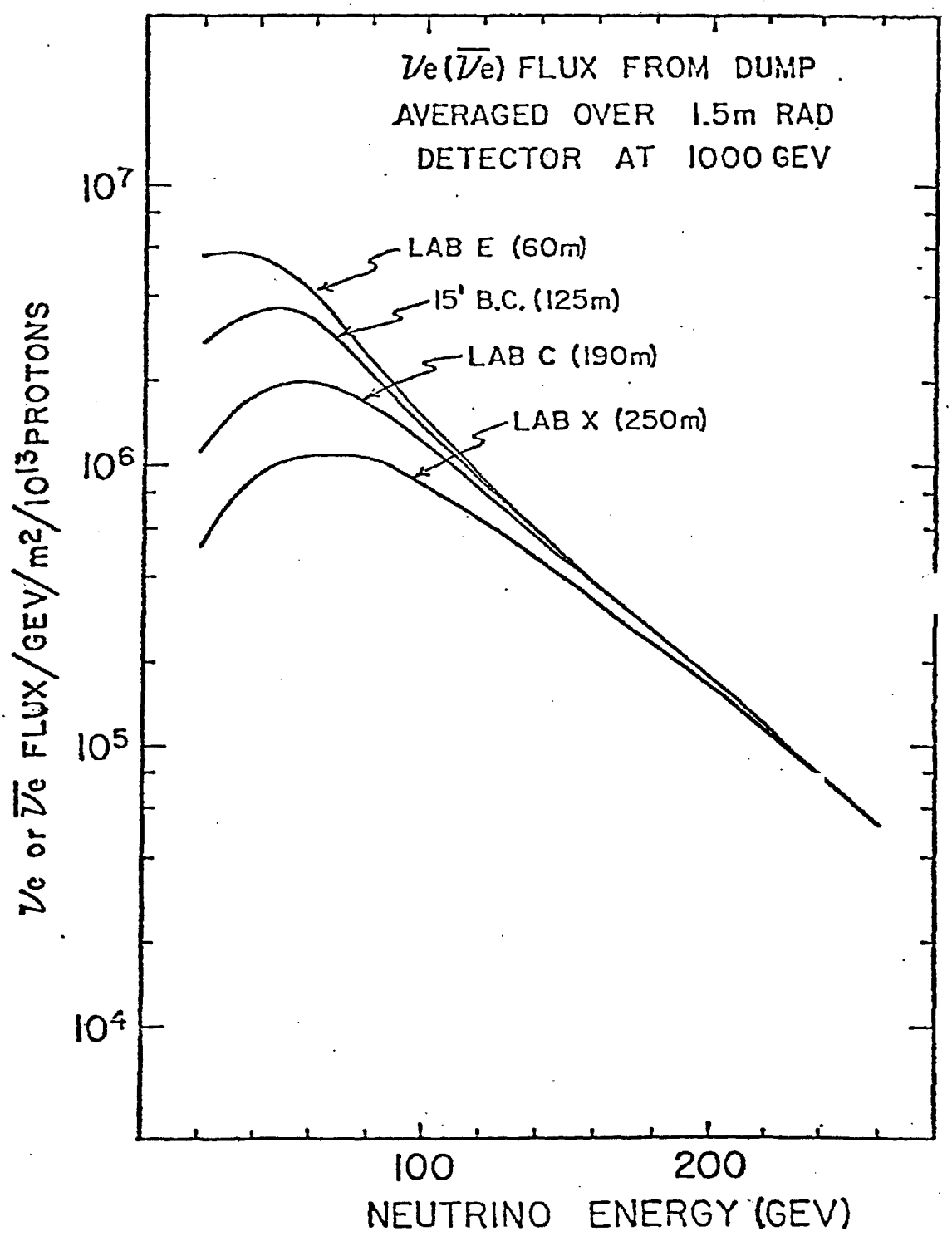
$\nu_e(\bar{\nu}_e)$ FLUX FROM DUMP
AVERAGED OVER 1.5m RAD
DETECTOR AT 1000 GEV
LAB E (60m)
15' B.C. (125m)
LAB C (190m)
LAB X (250m)
10^7
10^6
10^5
10^4
ν_e or $\bar{\nu}_e$ FLUX/GEV/m²/10^{13}PROTONS
100
200
NEUTRINO ENERGY (GEV)

Figure 1

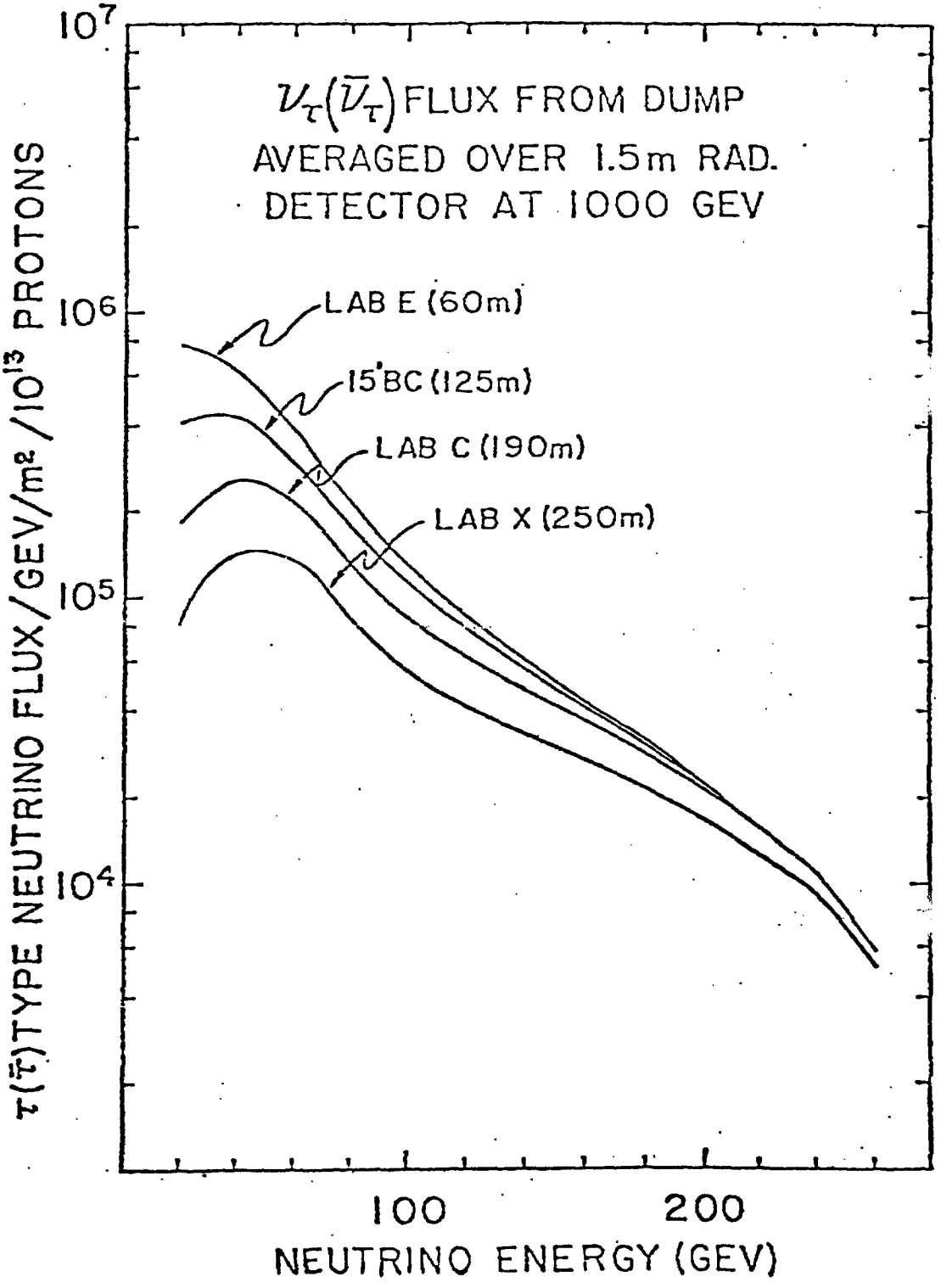
$\nu_\tau(\bar{\nu}_\tau)$ FLUX FROM DUMP
AVERAGED OVER 1.5m RAD.
DETECTOR AT 1000 GEV
LAB E (60m)
15°BC (125m)
LAB C (190m)
LAB X (250m)
10^7
10^6
10^5
10^4
$\tau(\bar{\tau})$ TYPE NEUTRINO FLUX/GEV/m^2/10^{13} PROTONS
100
200
NEUTRINO ENERGY (GEV)

Figure 2

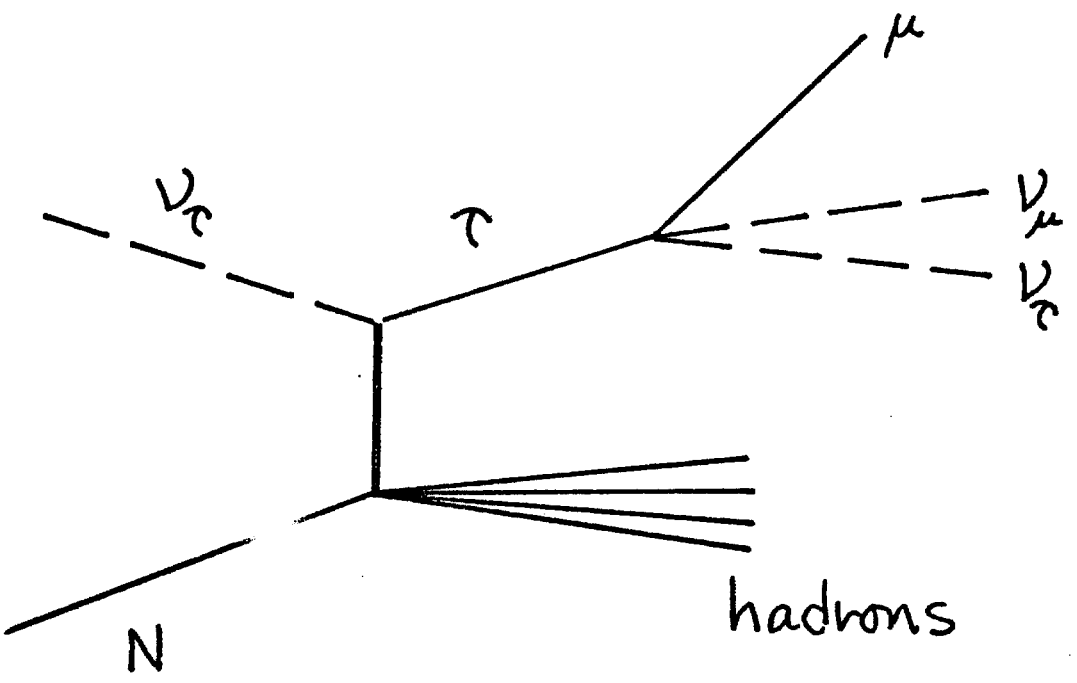
μ
ν_τ
τ
ν_μ
ν_τ
hadrons
N

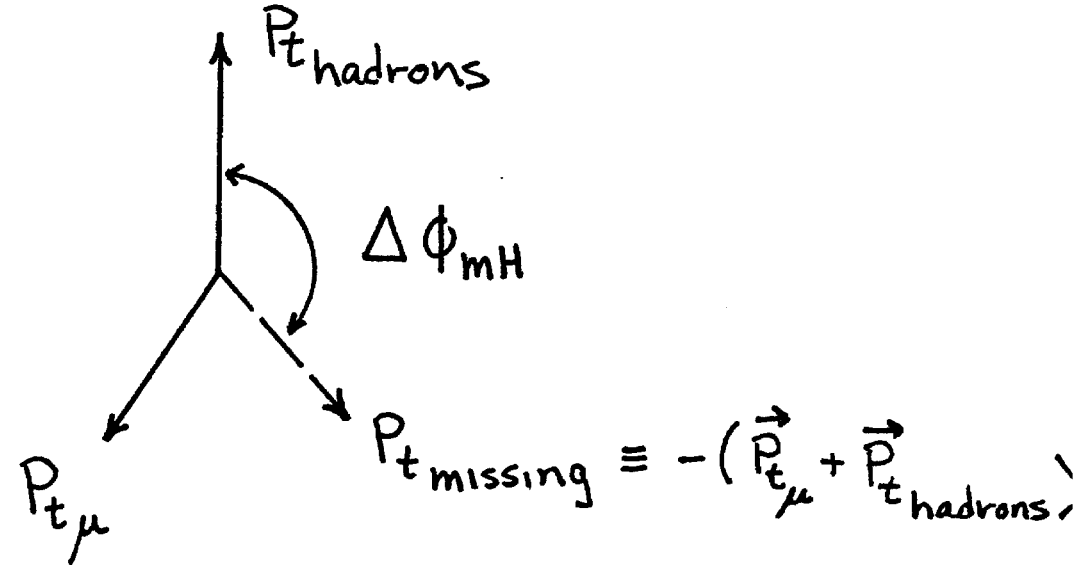
$P_{t_{hadrons}}$
$\Delta\phi_{mH}$
P_{t_μ}
$P_{t_{missing}} \equiv -(\vec{P}_{t_\mu} + \vec{P}_{t_{hadrons}})$

Figure 3

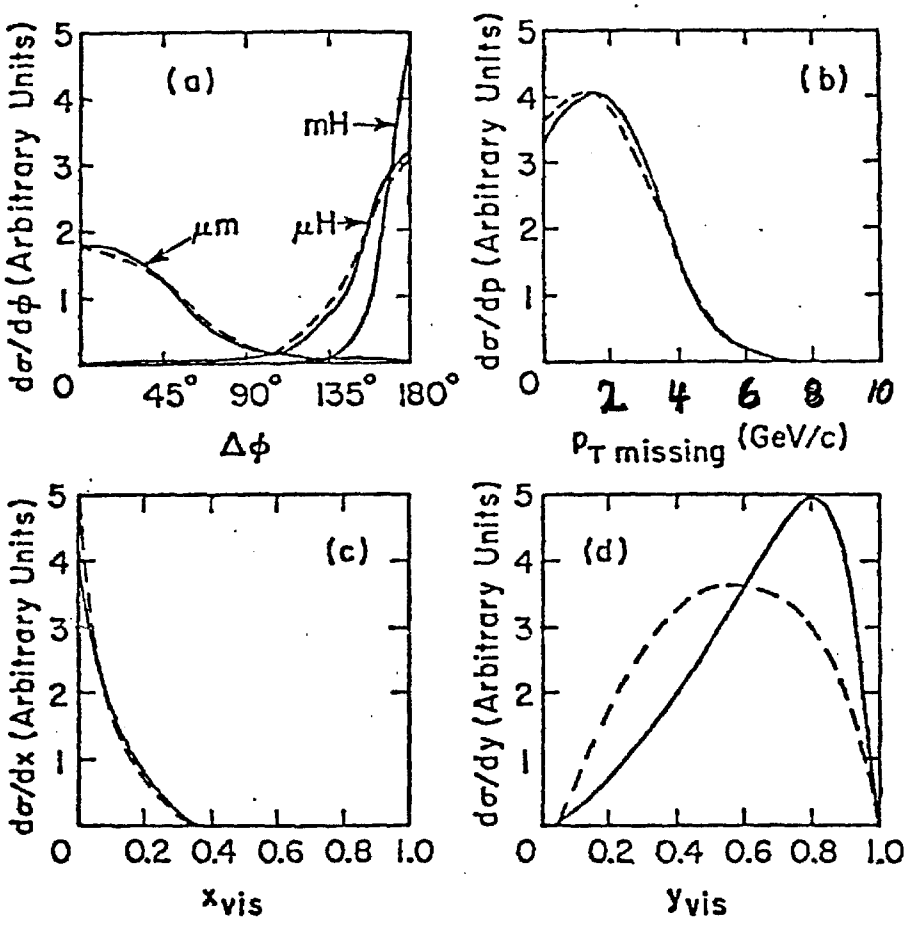
(a)
mH
μm
μH
dσ/dφ (Arbitrary Units)
0
1
2
3
4
5
45°
90°
135°
180°
Δφ
(b)
dσ/dp (Arbitrary Units)
2
4
6
8
10
pT missing (GeV/c)
(c)
dσ/dx (Arbitrary Units)
0.2
0.4
0.6
0.8
1.0
xvis
(d)
dσ/dy (Arbitrary Units)
yvis

Figure 4

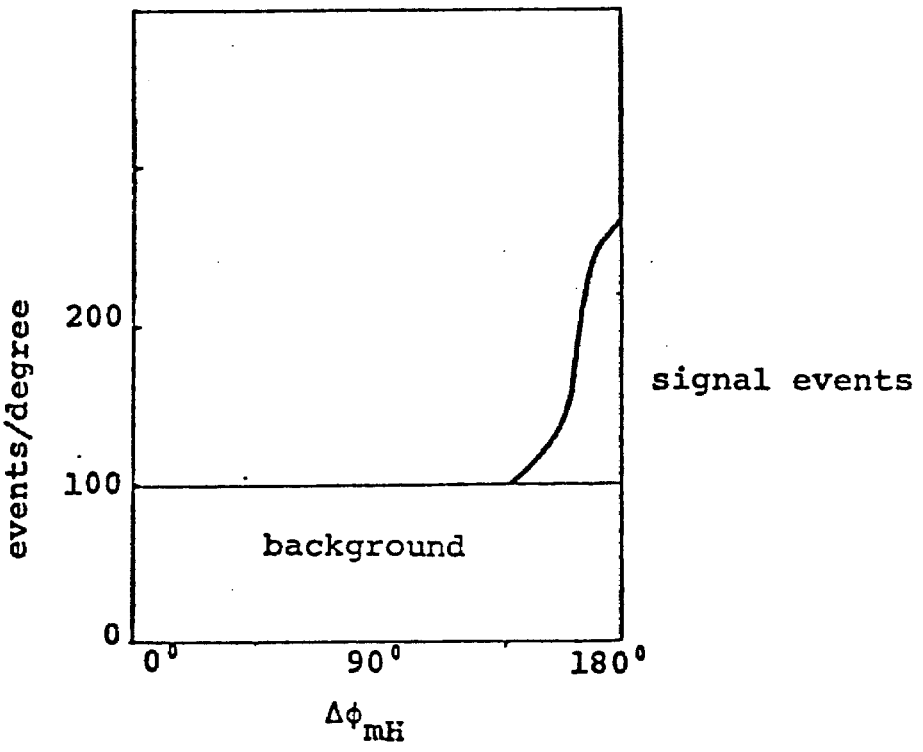
events/degree
200
100
0
background
signal events
0°
90°
180°
$\Delta\phi_{mH}$

Figure 5

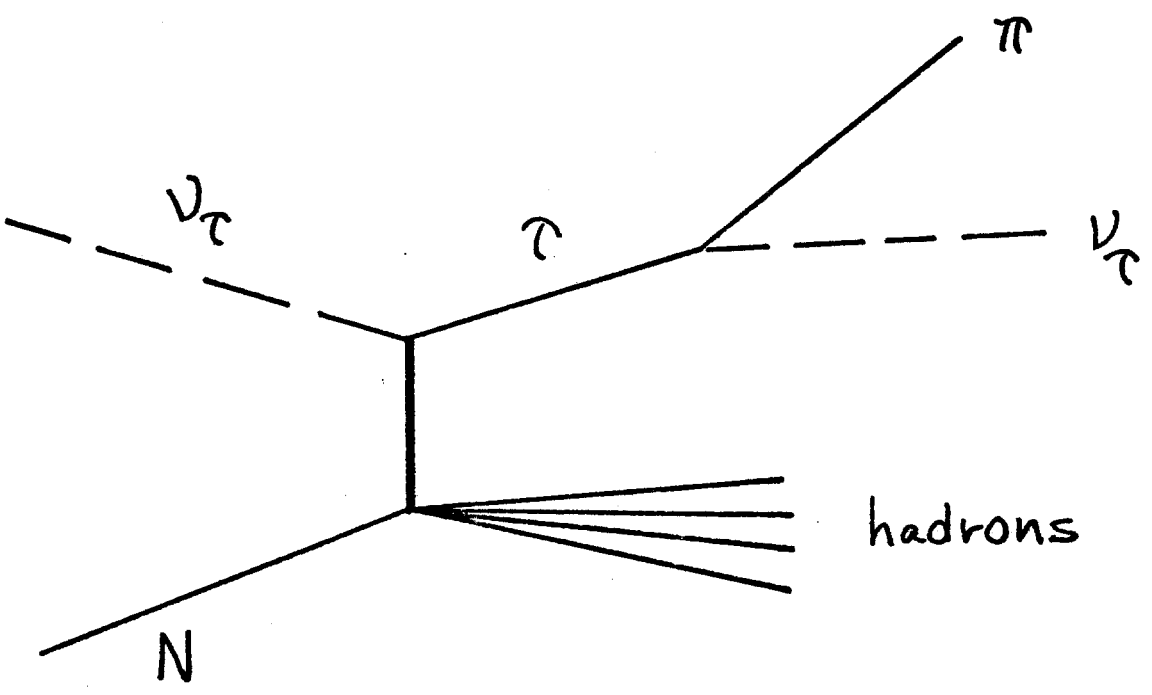

Figure 6

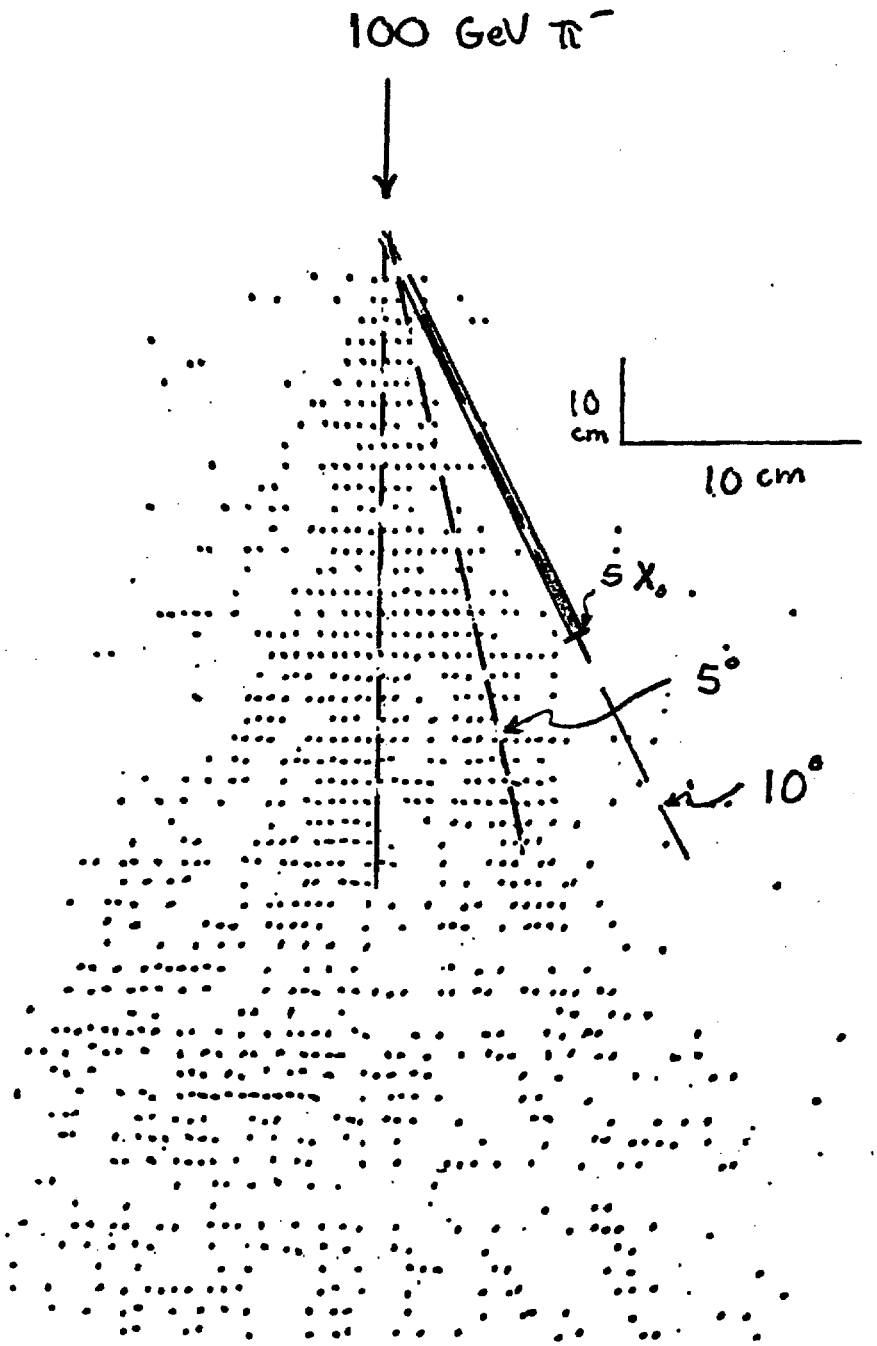

Figure 7

APPENDIX A: THE APPARATUS

I. INTRODUCTION

The Lab C flash chamber - proportional tube calorimeter is well suited for Tevatron era neutrino physics. It is ideal for studying neutral and charged current interactions, ν-e scattering and beam dump ν_τ physics. The calorimeter is fine grained (~400,000 flash tube cells) with a sampling step every 3% of an absorption length and 22% of a radiation length. It can distinguish electromagnetic from hadronic showers and has good energy and angular resolution for both. It has an excellent pattern recognition capability. Good muon momentum resolution at Tevatron energies is achieved by the 24' and 12' iron toroids which will be instrumented with drift chambers.

II. DESCRIPTION OF THE CALORIMETER

A. Arrangement of the Calorimeter

The flash chamber - proportional tube calorimeter is 60 feet (18 meters) long comprising 340 metric tons (see Fig. 1). The flash chambers are arranged in three views (X, Y and U) with cells which run 0°, 80° and 100° relative to horizontal (see Fig. 2). Each flash chamber is sandwiched by a sand plane and a steel shot plane. These target-absorber planes are made from extruded acrylic plastic sheets with 5/8" x 5/8" x 12' vertical cells filled with either sand or steel shot. Table I shows the arrangement of the target-absorber planes within the flash chambers and lists the corresponding absorption and radiation

lengths. The proportional tube planes are located one every 16 flash chambers. Hence between adjacent proportional planes are 0.5 absorption lengths (64 g/cm^2) or 3.5 radiation lengths. The proportional tubes are alternately vertical and horizontal.

B. General Properties

The average density of the calorimeter is 1.40 g/cm^3. The average nuclear charge Z is 19.1. This low average Z was obtained by using sand as a part of our target-absorber and allows us to measure the angle of electromagnetic showers well. The average collision, absorption and radiation lengths in the calorimeter are 51.8, 83.1 and 11.7 cm respectively. The size of hadronic showers in the calorimeter, or more precisely the dimensions required for containment of the shower energy, is given in Fig. 4. The curves in Fig. 4 were obtained using shower depth calculations in liquid scintillator by the HPWF group.[1] The hadronic shower resolutions, discussed later, demand at least 99% of the shower is contained in the calorimeter longitudinally and at least 95% laterally. The calorimeter properties are summarized in Table II.

C. The Flash Chambers

There are about 600 flash chambers, each with approximately 650 5 mm x 5 mm cells. This fine granularity of the flash chambers allows a small sampling step of the recoil showers leading to excellent energy and angle determination, pattern recognition and muon track finding. The flash chambers are made

of extruded black polypropylene with aluminum foil electrodes glued on both sides. Each flash chamber has an active area of 12' x 12' (3.66 m x 3.66 m). Standard spark chamber gas: 90% Ne, 10% He, is circulated through the cells.

When an event is detected, a high voltage pulse of 4.5 kV is applied across each chamber for 0.5 μsec. During this high voltage pulse, a plasma discharge is developed in the hit cells of the flash chambers. This plasma discharge propagates down the full 12' length of the flash chamber cell and into a read out region at the end of each cell. A copper strip for each cell is glued over this 2-ft long read out region and develops a current pulse when the cell is hit. The current pulse is then read out by magnetostrictive techniques.

D. The Proportional Tubes

The trigger and energy determination at large energies are provided by planes of proportional tubes. There are 37 such planes, each containing 144 tubes. The planes are made of extruded aluminum. Each tube is 1" x 1" x 12' and is strung with a single 2 mil gold plated tungsten wire. Four tubes are connected to one amplifier to reduce the cost of electronics while still maintaining adequate granularity for triggering purposes. An argon-ethane (50%-50%) gas mixture is used to give fast drift times ($\lesssim$200 ns) needed to form the trigger within the flash chamber sensitive time.

The trigger will be based on the total energy deposition and on the topology of the energy deposition. Discrimination

in the trigger between electromagnetic and hadronic showers will be accomplished using the shower length (the number of proportional planes hit) and the shower width (the separation of hit channels within a plane).

E. Scintillation Counters

Liquid scintillation counters with a 12' x 12' sensitive area are placed every 80 flash chambers throughout the calorimeter. The most upstream counter serves as a front wall veto counter. The other scintillation counters will be used for efficiency measurements and corroborative information on hadronic shower energy deposition. They will also provide time of flight information.

F. The Muon Spectrometer

The muon momentum for charged current interactions and multi-muon events will be measured in the muon spectrometer at the rear of the apparatus (see Fig. 1). There are three 24-ft diameter by 2-ft thick iron toroids immediately downstream of the calorimeter and four 12-ft diameter by 4-ft thick iron toroids behind these. The muons travel through the equivalent of approximately 13 kG in 5 meters of magnetized iron, corresponding to a $p_\perp$ kick of about 2 GeV/c.

The toroids are instrumented with scintillation counters to supply trigger information regarding the presence or absence of a muon in the toroids. Behind each of the seven toroids will be four planes of drift tubes. The planes are made of

extruded aluminum, each tube having a 1" x 1" cross section. Two of the four planes will have vertical tubes: the tubes of one plane being offset one-half of a tube with respect to those of the other plane to resolve right-left ambiguities. The other two planes of the set of four will have horizontal tubes.

III. RESOLUTIONS

A. Energy Resolution

The hadronic shower energy is measured by the flash chambers at low energies and the proportional tubes at high energies (see Fig. 4). Because of their fine grained sampling, the flash chambers provide good resolution as low as 10 GeV. At high energies (above 200 GeV), where multiple hits per cell degrade the flash chamber resolution, the proportional tubes provide a good energy measurement. Figure 5 shows the electromagnetic shower energy resolution determined only by the flash chambers. For both kinds of showers, the flash chamber energy measurement is determined by cell counting. The proportional tube energy measurement is determined by summing the analog signals from all the wires.

The preliminary flash chamber energy resolutions in Figs. 4 and 5 were directly measured in a hadron and electron beam using our test calorimeter.[2] The test calorimeter was made with plastic flash chambers, smaller in size and number than our Lab C chambers, and read out optically. The longitudinal sampling of the test calorimeter: 3.5% λ_{abs} and 24% X_o, was almost as good as

the Lab C calorimeter. Therefore only corrections for the limited hadronic shower containment of the test calorimeter were made to the measured resolutions. The proportional tube resolution of Fig. 4 was estimated by scaling Anderson et al.[3] to our sampling step, giving

$$\frac{\sigma(E_h)}{E_h} \cong \frac{104\%}{\sqrt{E_h}}$$

B. Angular Resolution

The hadronic and electromagnetic shower angular resolutions determined by the test flash chamber calorimeter are shown in Figs. 6 and 7. The angular resolutions depend critically on the spatial resolution of the shower vertex. The angle of the showers is computed by first locating the vertex and then using the "center of gravity" of the shower as a function of shower depth.

Because every cell of the test calorimeter ran horizontal, the sampling step per view was approximately a factor of two finer in the test calorimeter than in the Lab C calorimeter. By ignoring every other plane in the test calorimeter's angle measurement, therefore, we were able to plot the expected angular resolution of the Lab C calorimeter. The test calorimeter confirmed the expectation of good angular resolution at low energies: an important feature for beam dump physics. Figure 8 shows test calorimeter showers at all energies. Note the good vertex determination even at low energies.

C. Pattern Recognition

We will be able to distinguish electromagnetic from hadronic showers by their size, shape and structure. This is an important capability for the study of ν-e scattering where hadronic backgrounds are large. As seen in the test calorimeter showers of Fig. 8, electromagnetic showers are easily distinguished from high energy hadronic showers by differences in their size. We distinguish low energy hadronic from electromagnetic showers by the presence of large angle secondaries in the hadronic showers. Also, unlike electromagnetic showers, tracks are visible within the hadronic showers. Using the test calorimeter in a hadron beam with about 1% electron contamination, we were able to experimentally confirm that less than 1% of hadron showers are misidentified as electron showers.

We will also be able to observe and locate the muon track in charged current interactions. We expect a very small amount of charged current interactions posing as neutral current interactions because the muon could not be seen.

D. Muon Momentum Resolution

Figure 9 shows the muon momentum resolution we expect to achieve when the 24 and 12-ft iron toroids are instrumented with drift tubes. The drift tubes will provide position measurements with an estimated σ of 1 mm. The flash chambers will supply information regarding the muon's trajectory at the point of entry into the first toroid. The resolutions corresponding to the drift tube and flash chamber position measurements, as well as multiple scattering were used to produce the resolution shown.

IV. PERFORMANCE OF THE CALORIMETER

A. Flash Chamber Performance

We have debugged and operated 320 flash chambers. From our experience we find that the flash chambers have performed well.[4] Using cosmic ray muons, we have measured their efficiency at the proportional tube trigger time delay (650 ns from the event to the time high voltage appears across the chambers) to be between 80 and 90%. The multiplicity (cells lit per flash chamber per cosmic ray) is 1.3. Adequate recirculation of the neon-helium gas was found to be 1.5% of the volume per minute. For the entire detector, this implies a recirculation rate of 900 liters per minute. The high voltage plateau region is broad: 3.5 to 5.5 kV (see Fig. 10). The signal-to-noise ratio of the amplified signals on the magnetostrictive lines is 10:1. Our maximum repetition rate with almost no cell reignition thus far is ~1 flash per second. We have not added any electronegative gas to try to improve this.[5] The readout dead time (up to the computer) is ~70 ms. Because data transfer time to the disk is 50,000-80,000 words per second, the computer cannot handle much more than one event per second. If we wanted to take data at a faster rate, we could transfer data without the disk by obtaining much more addressable core memory (such as a VAX) or by using a 6250 BPI tape drive.

Figure 11 shows a cosmic ray muon in 160 of our chambers. (Offline alignment corrections have not yet been made.) In Fig. 12, a cosmic ray muon initiated an electromagnetic shower. In Fig. 13, which shows a cosmic ray muon interacting, 320 of our chambers were in operation.

B. Proportional Tube Performance

The proportional tubes have also performed well. Using 50% argon - 50% ethane gas and running at a high voltage of 2000 volts gives us a gas gain of about 2000 and drift times of $\lesssim$200 ns. The amplifier gain is 1 mV/fC. A minimum ionizing particle gives a signal of 8 mV: a factor of 8 above noise. The linear swing is 0-4 volts or 0-500 particles. This is a factor of 2 or so above the largest number of particles per channel expected for Tevatron energy showers. The tube to tube uniformity has been measured to be very good: a plot of Cd^{109} peaks for a large sample of tubes shows a σ of $\lesssim$5%.

V. CONCLUSION

The flash chamber - proportional tube calorimeter is a high tonnage, fine grained device with good energy and angle resolutions for both hadronic and electromagnetic showers. It has a good hadronic-electromagnetic shower distinction capability and a low average Z, making it ideal for the study of ν-e scattering. Its good vertex determination and good muon momentum resolution make it ideal for studying charged and neutral current interactions. Its good pattern recognition and angle determination at low energies make it an excellent beam dump detector. It will be a powerful device for studying a number of interesting physical processes at Tevatron energies.

REFERENCES

1. F. J. Sciulli, Proceedings of the Calorimeter Workshop (Fermilab), 79 (1975).

2. See Appendix A of the E594 Proposal (February 1978) and F. E. Taylor et al., IEEE Trans. Nucl. Sci. NS-25, 312 (1978).

3. R. L. Anderson et al., IEEE Trans. Nucl. Sci. NS-25, 340 (1978) and private communication with D. M. Ritson.

4. F. E. Taylor et al., IEEE Trans. Nucl. Sci. NS-27, 30 (1980).

5. Chaney and Breare, by adding 1% methane to the neon-helium, have been able to pulse their flash chambers at 50 Hz with no reignition. See J. E. Chaney and J. M. Breare, Nucl. Instrum. and Methods 124, 61 (1975).

TABLE I

Arrangement of Calorimeter Components

flash chambers:	U	X	Y	X	. . .
	↑	↑	↑	↑	
absorber planes:	shot	sand	shot	sand	
absorption lengths:	3.7%	2.5%	} 6.1% per view ($7.2\ g/cm^2$)		
radiation lengths:	36%	8%	} 44% per view		

TABLE II

General Properties

Tonnage:	340 metric tons
Fiducial Tonnage for a Neutral Current Experiment:	100 metric tons
Fiducial Tonnage for a ν-e Scattering Experiment:	225 metric tons
Average Density:	1.40 g/cm^3
Average Z:	19.1
Average λ_{COL}:	51.8 cm
λ_{ABS}:	83.1 cm
X_o:	11.7 cm

LIST OF FIGURES

E-594 CALORIMETER

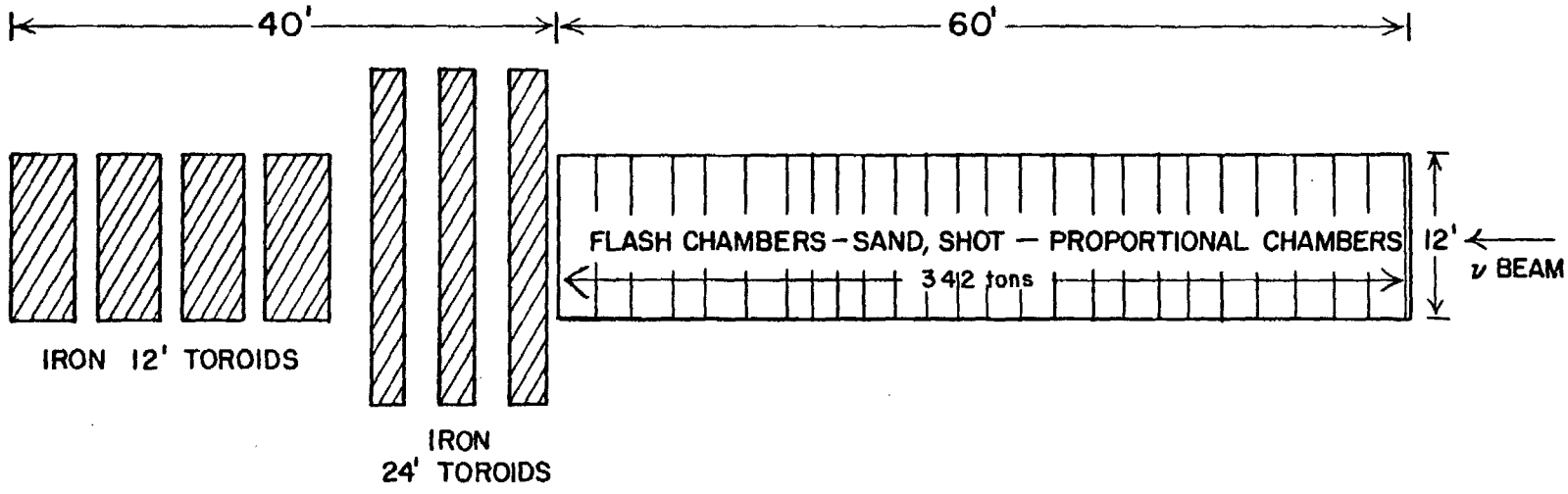

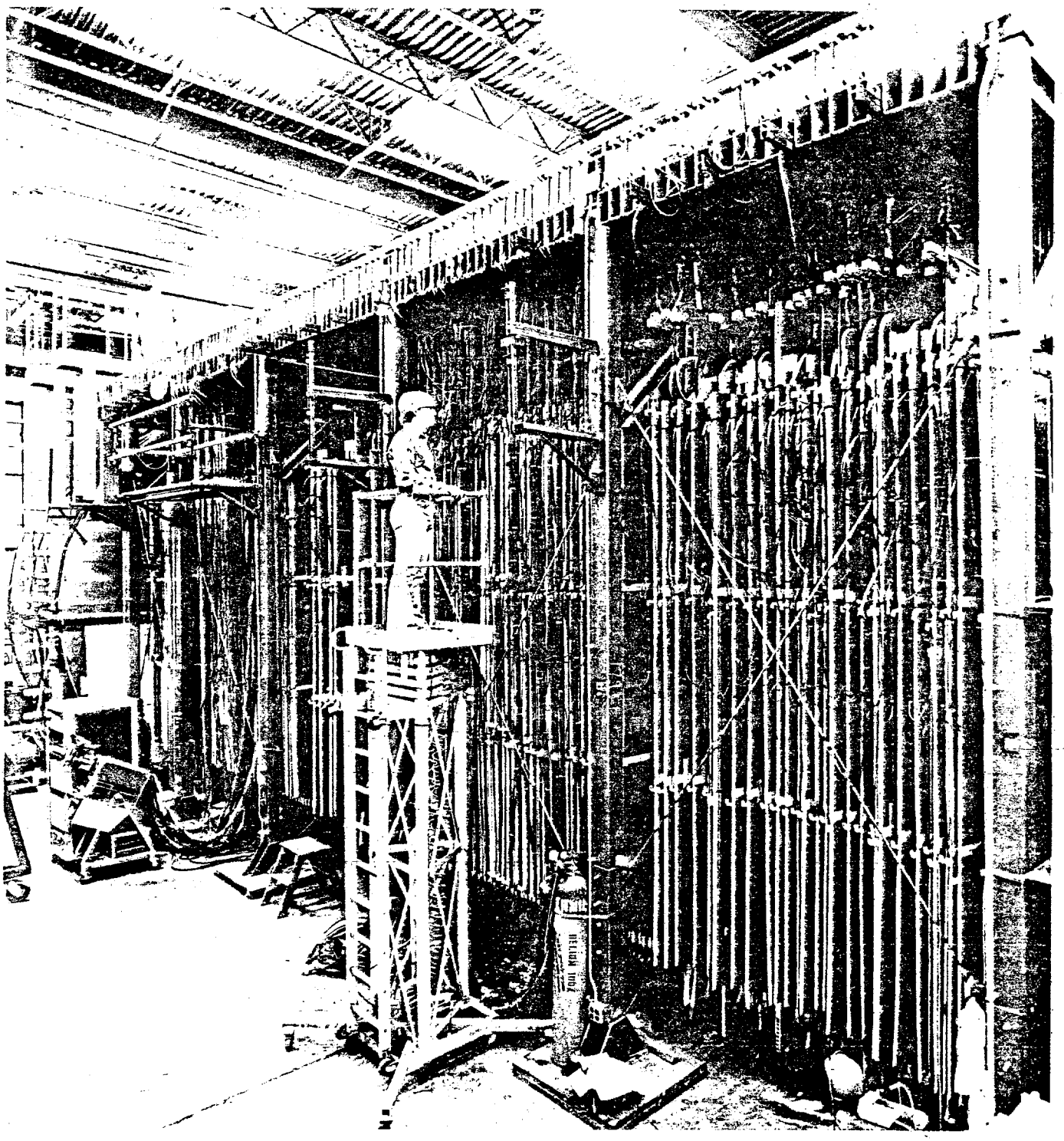

Figure 1b

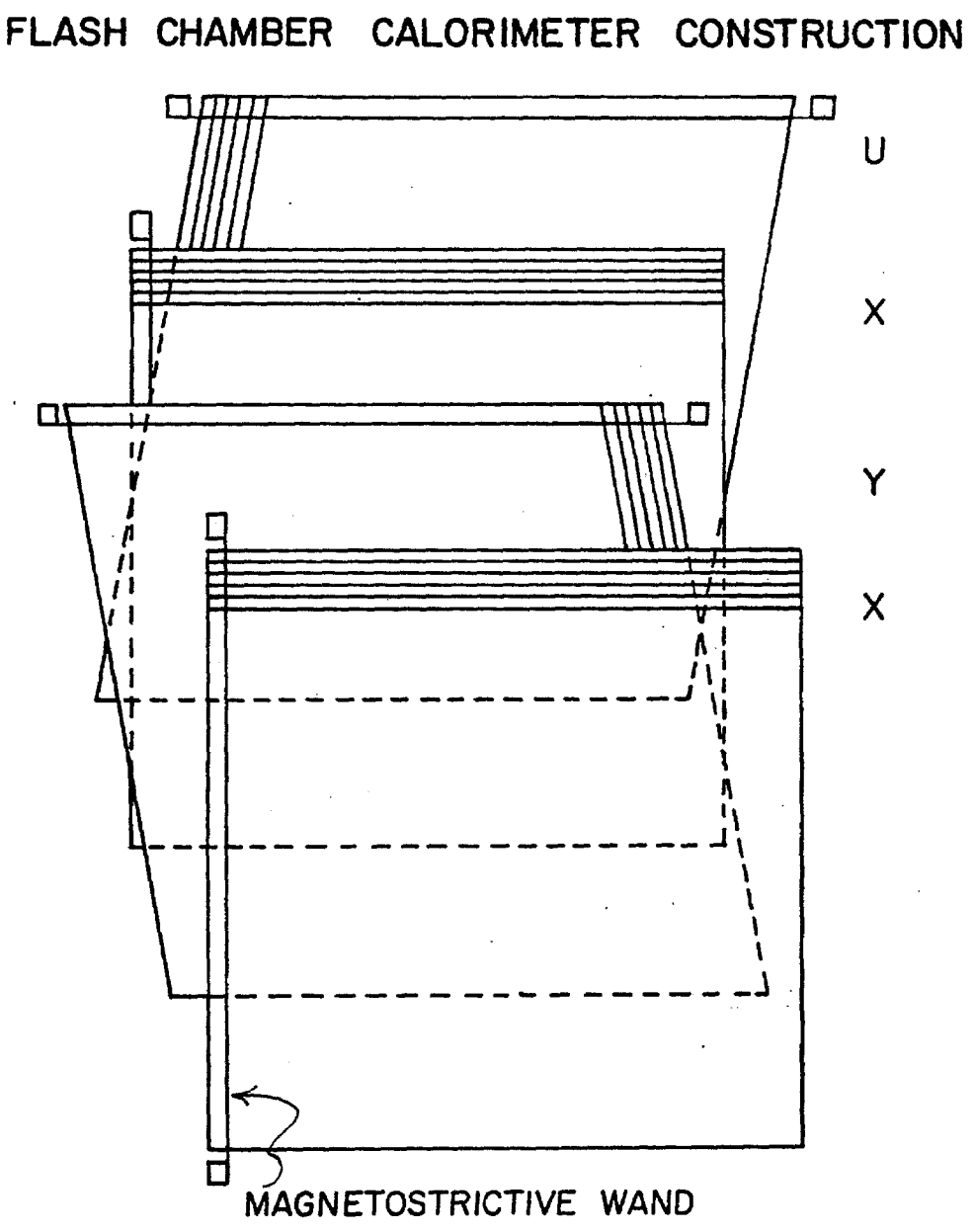
FLASH CHAMBER CALORIMETER CONSTRUCTION
U
X
Y
X
MAGNETOSTRICTIVE WAND

Figure 2

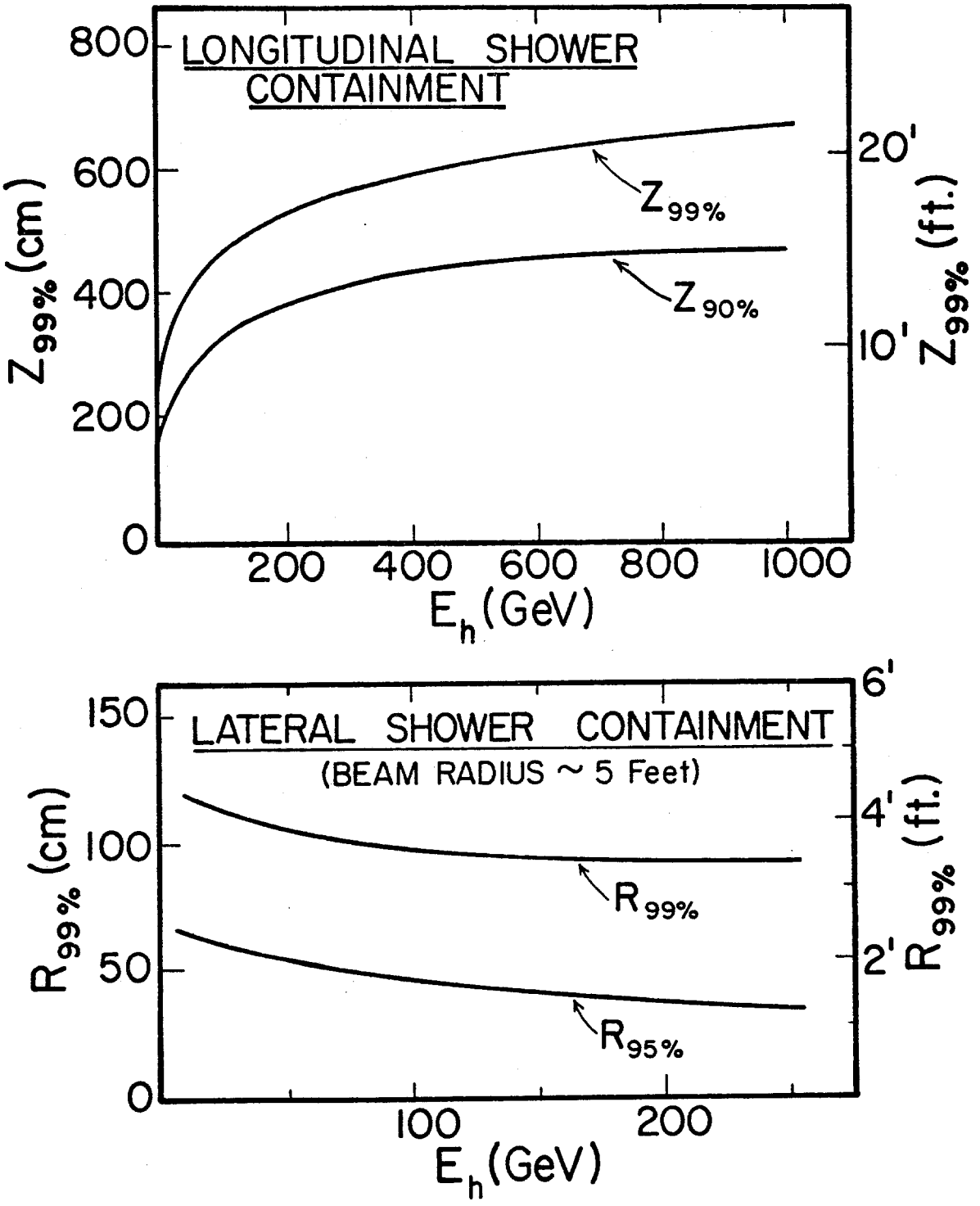
LONGITUDINAL SHOWER CONTAINMENT
800
600
400
200
0
$Z_{99\%}$ (cm)
20'
10'
$Z_{99\%}$ (ft.)
$Z_{99\%}$
$Z_{90\%}$
200
400
600
800
1000
E_h (GeV)
LATERAL SHOWER CONTAINMENT
(BEAM RADIUS ~ 5 Feet)
150
100
50
0
$R_{99\%}$ (cm)
6'
4'
2'
$R_{99\%}$ (ft.)
$R_{99\%}$
$R_{95\%}$
100
200
E_h (GeV)

Figure 3

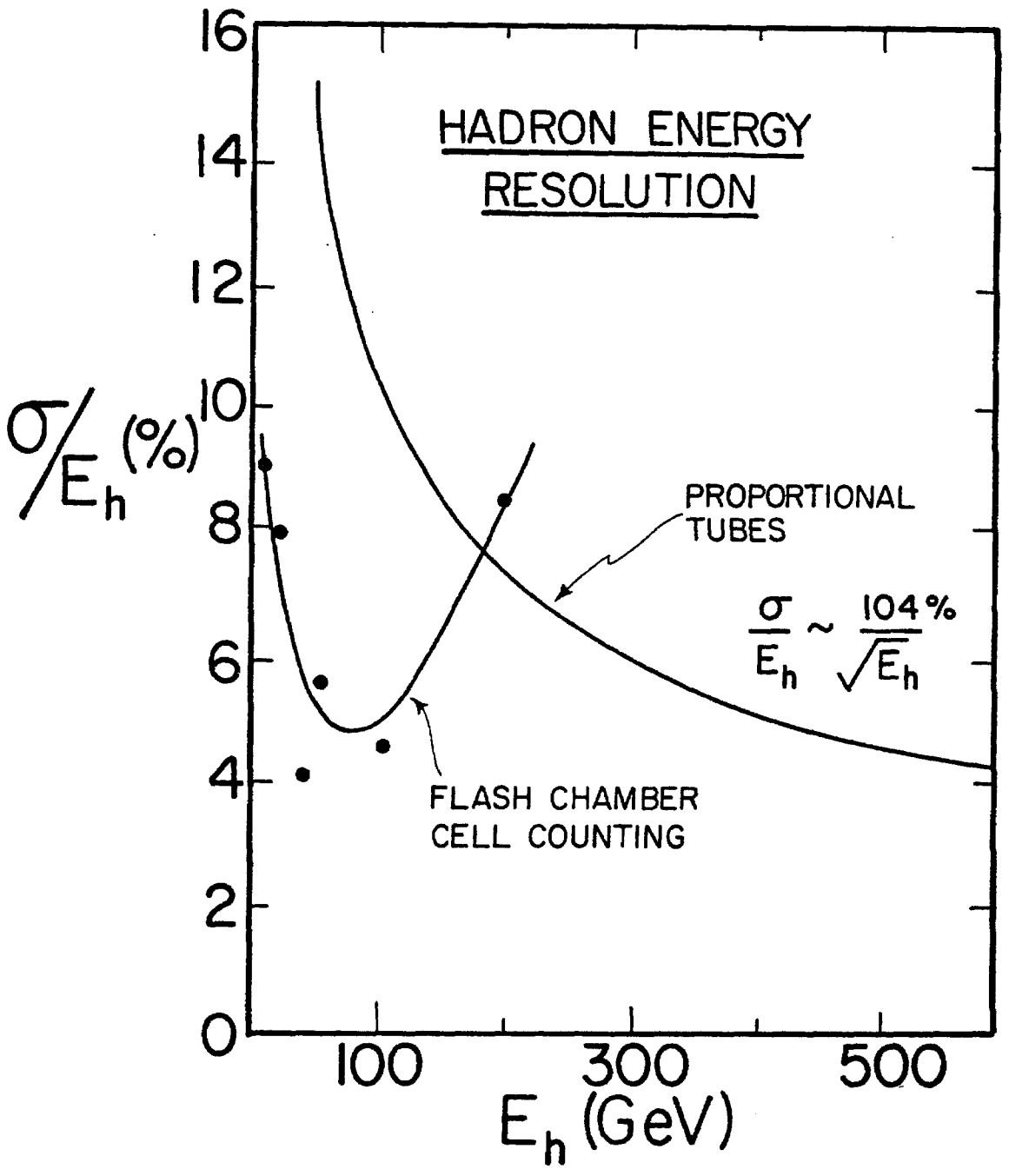
HADRON ENERGY
RESOLUTION
PROPORTIONAL
TUBES
$\frac{\sigma}{E_h} \sim \frac{104\%}{\sqrt{E_h}}$
FLASH CHAMBER
CELL COUNTING
σ/E_h (%)
E_h (GeV)
0
2
4
6
8
10
12
14
16
100
300
500

Figure 4

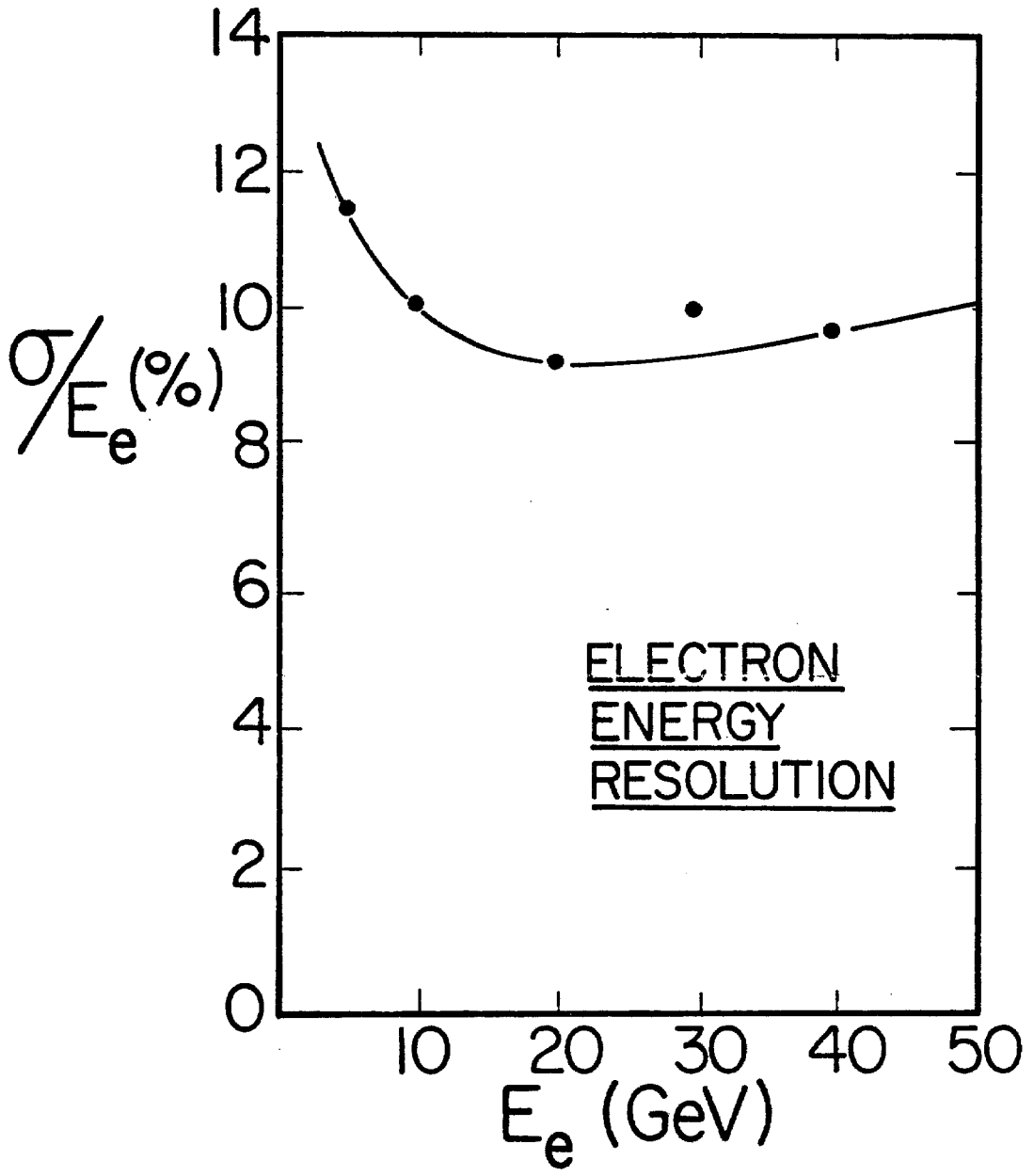
14
12
10
8
6
4
2
0
σ/E_e (%)
ELECTRON
ENERGY
RESOLUTION
10
20
30
40
50
E_e (GeV)

Figure 5

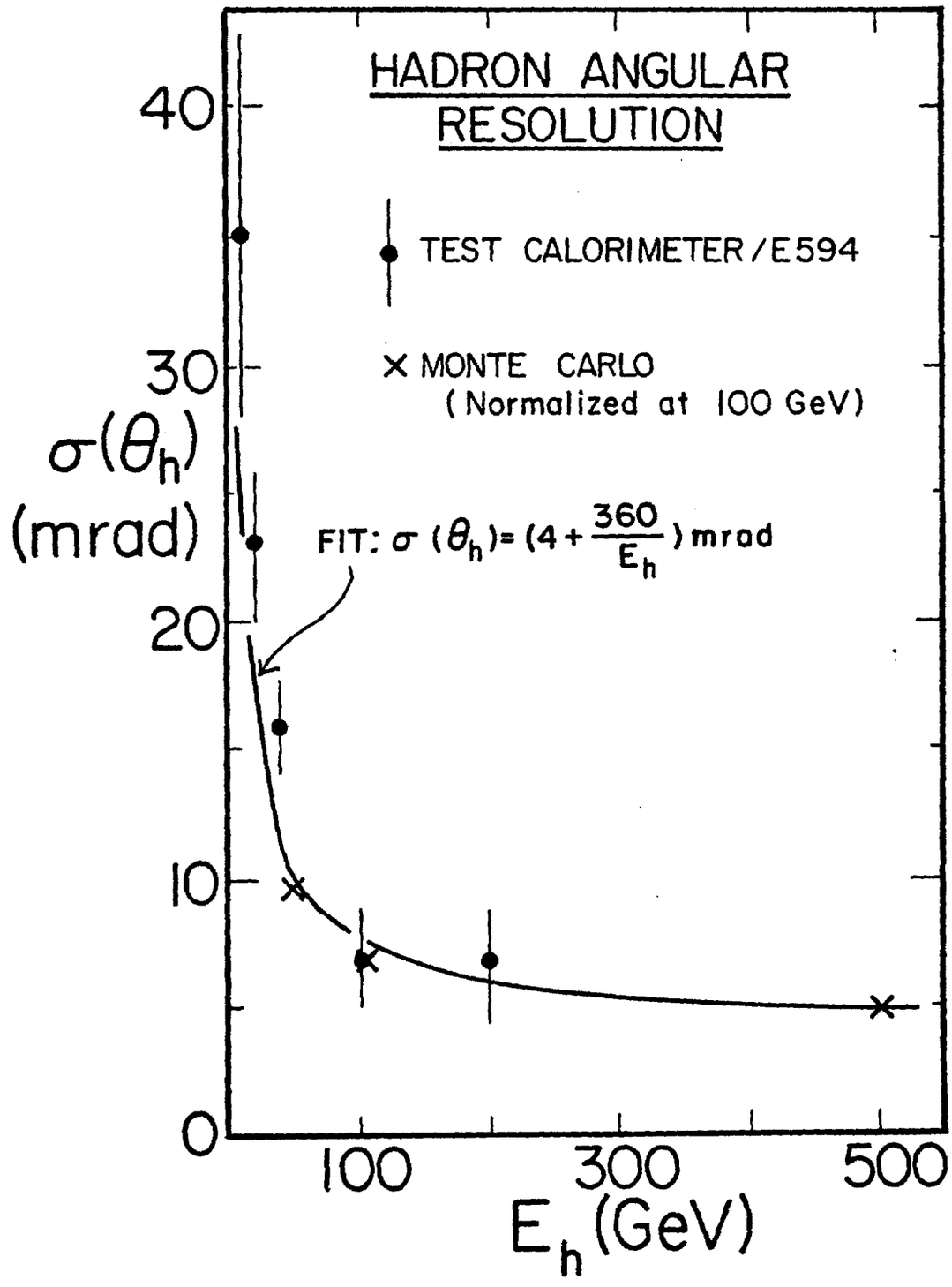
HADRON ANGULAR RESOLUTION
TEST CALORIMETER / E594
× MONTE CARLO
(Normalized at 100 GeV)
FIT: σ (θh) = (4 + 360/Eh) mrad
σ(θh) (mrad)
40
30
20
10
0
100
300
500
Eh (GeV)

Figure 6

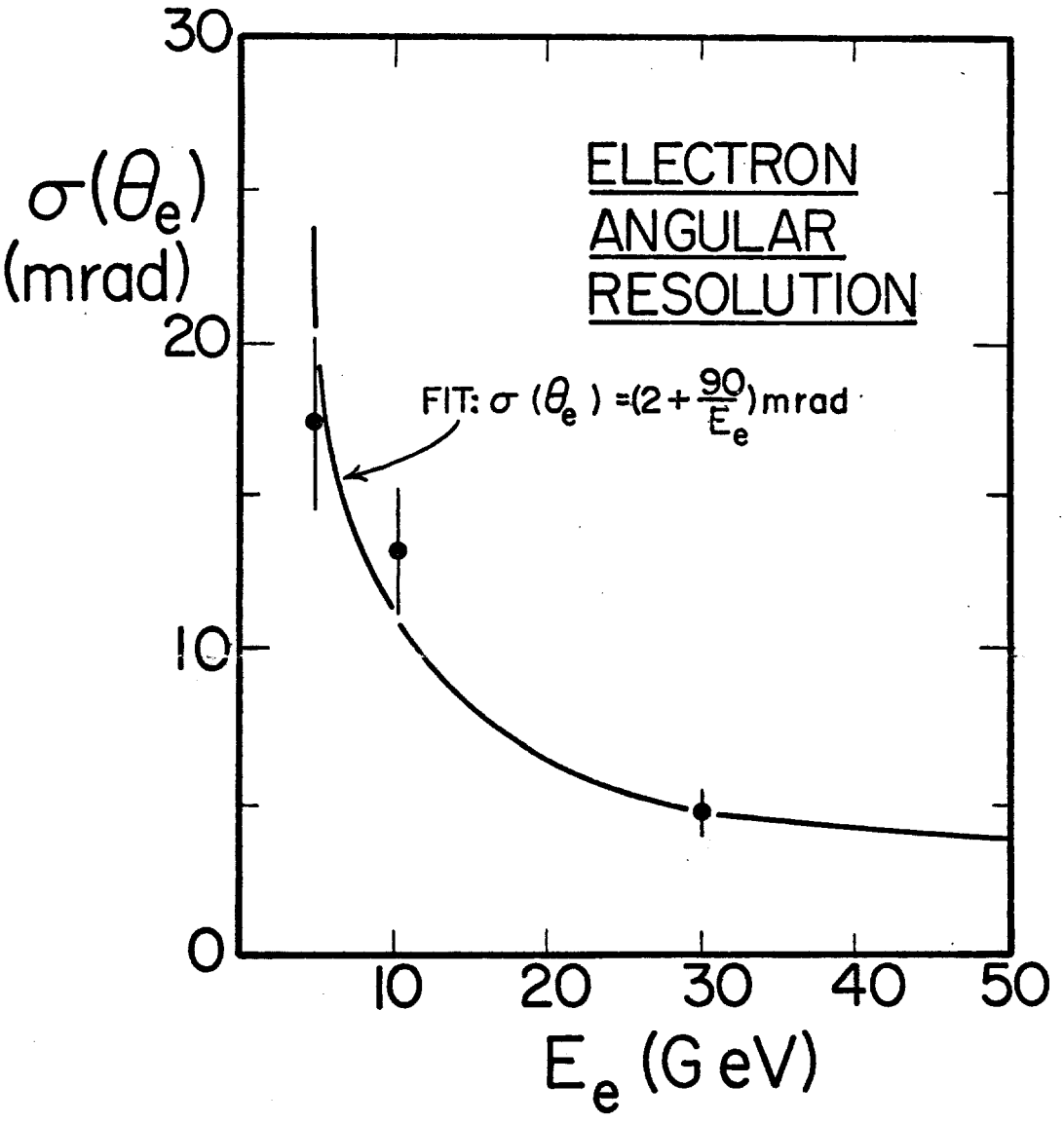
30
20
10
0
σ(θe)
(mrad)
ELECTRON
ANGULAR
RESOLUTION
FIT: σ (θe) =(2+90/Ee)mrad
10
20
30
40
50
Ee (GeV)

Figure 7

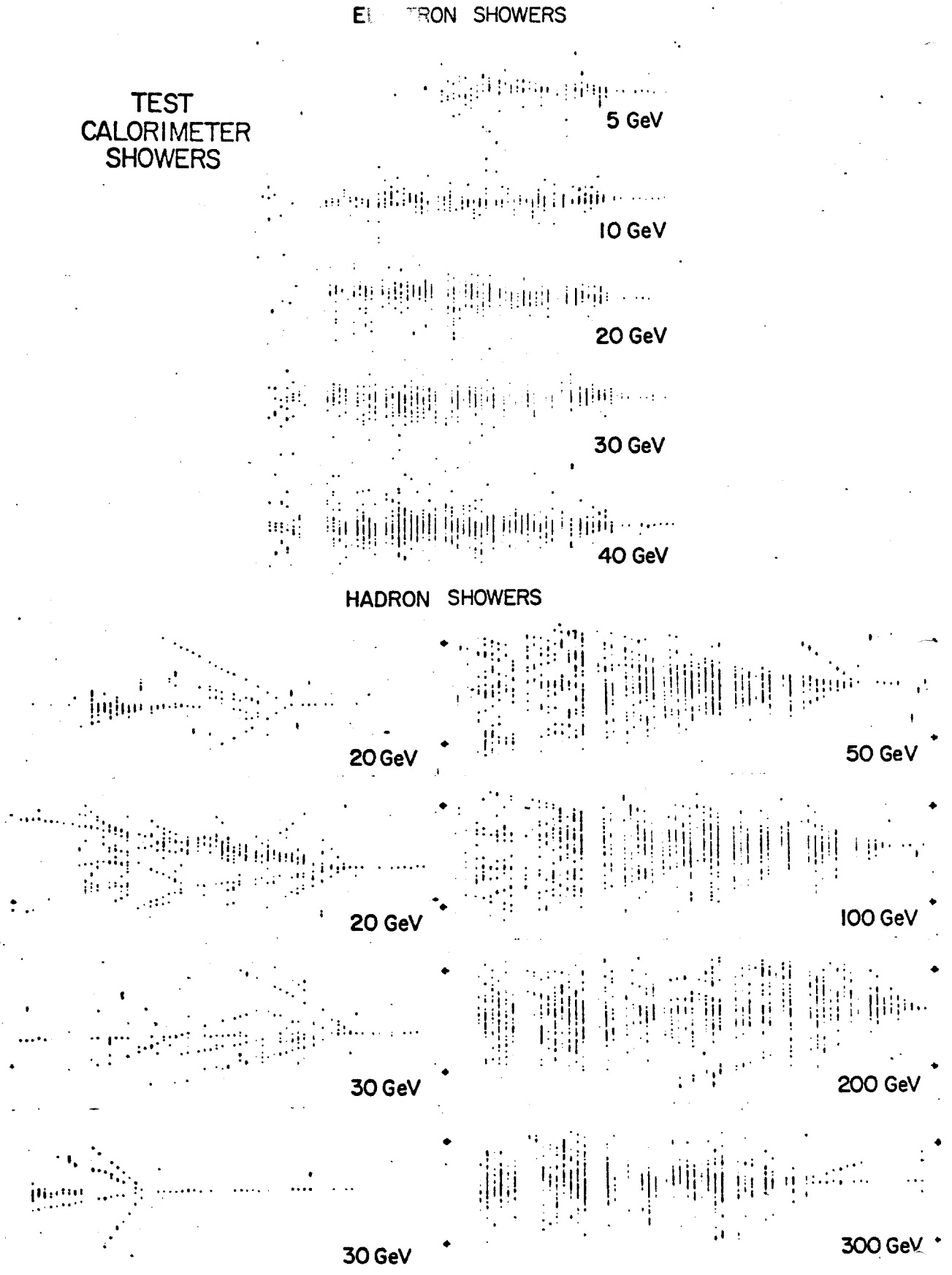
E TRON SHOWERS
TEST
CALORIMETER
SHOWERS
5 GeV
10 GeV
20 GeV
30 GeV
40 GeV
HADRON SHOWERS
20 GeV
50 GeV
20 GeV
100 GeV
30 GeV
200 GeV
30 GeV
300 GeV

Figure 8

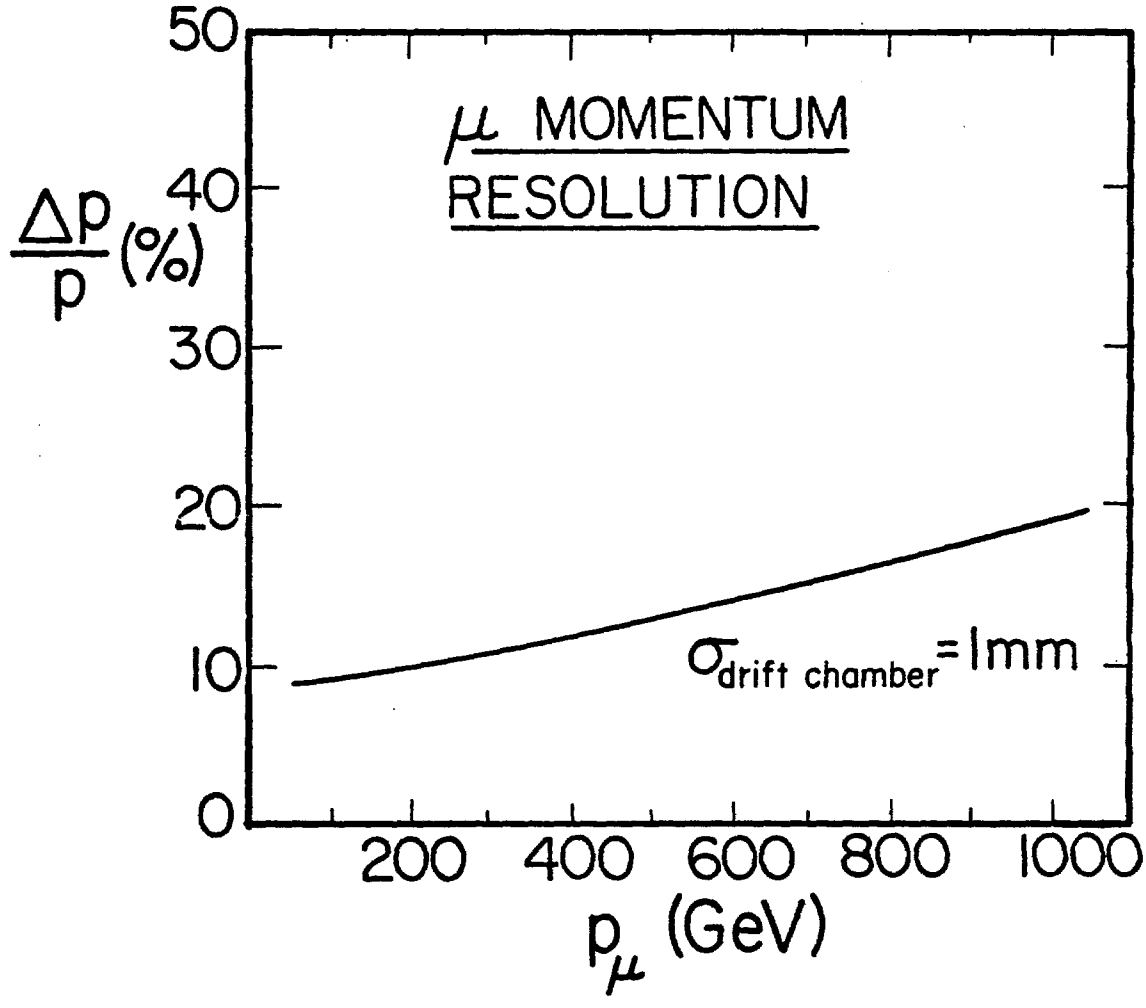
μ MOMENTUM
RESOLUTION
Δp/p (%)
50
40
30
20
10
0
σdrift chamber = 1mm
200
400
600
800
1000
pμ (GeV)

Figure 9

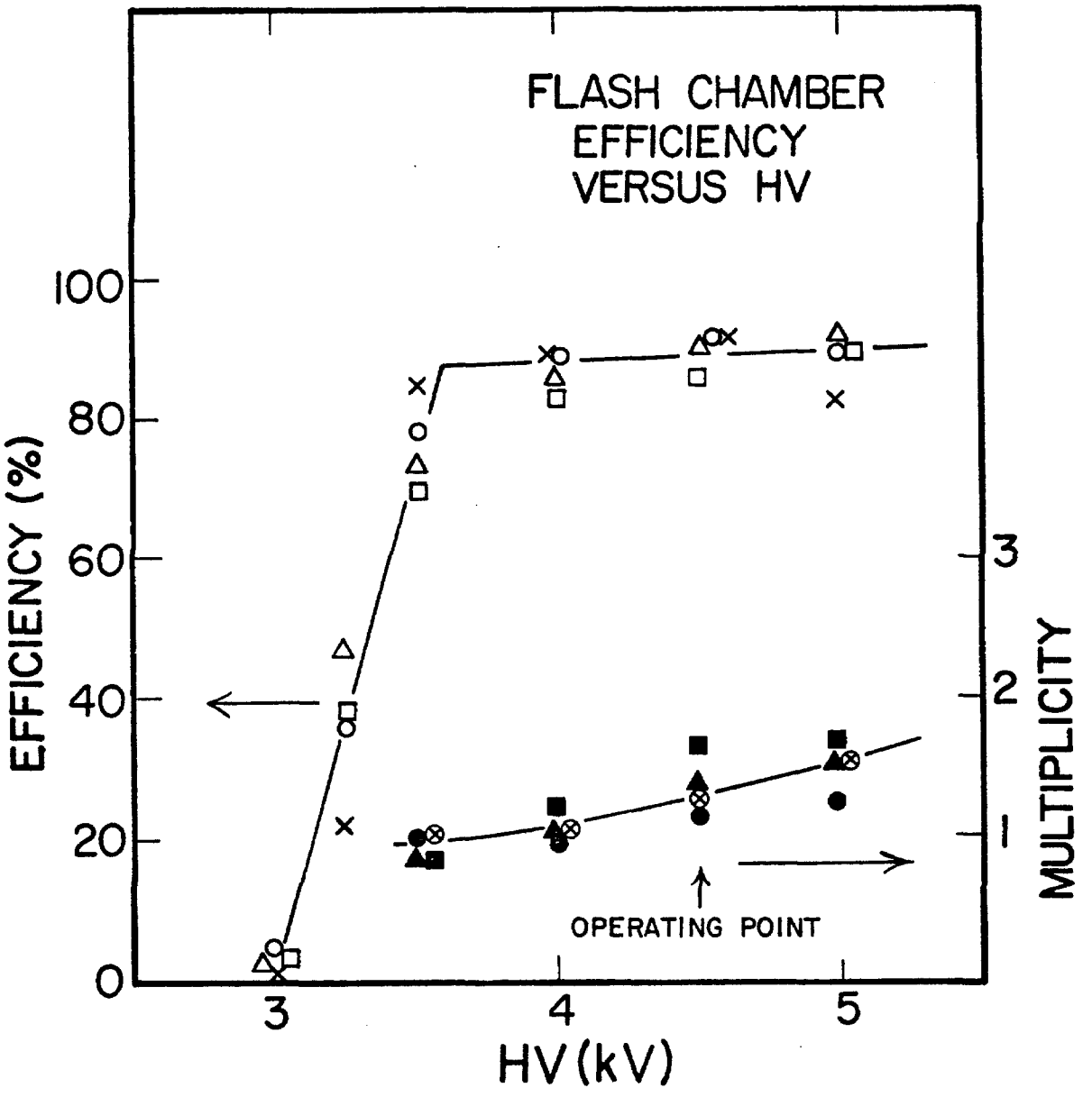
FLASH CHAMBER
EFFICIENCY
VERSUS HV
EFFICIENCY (%)
MULTIPLICITY
HV (kV)
OPERATING POINT
0
20
40
60
80
100
1
2
3
3
4
5

Figure 10

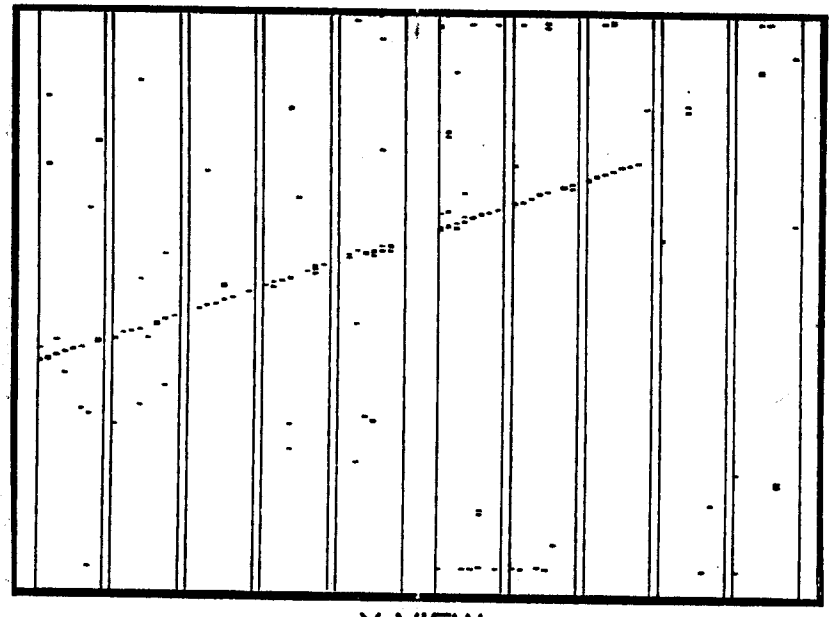

X VIEW

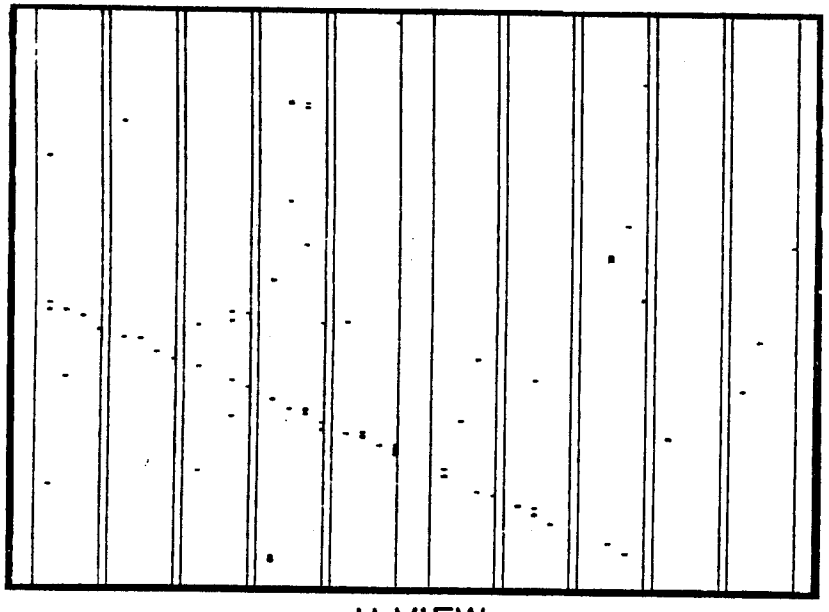

U VIEW

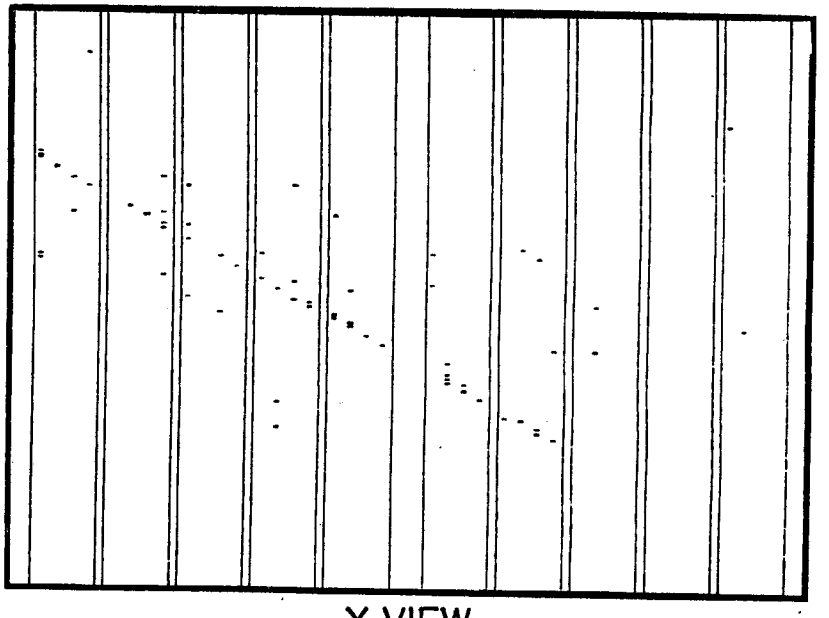

Y VIEW

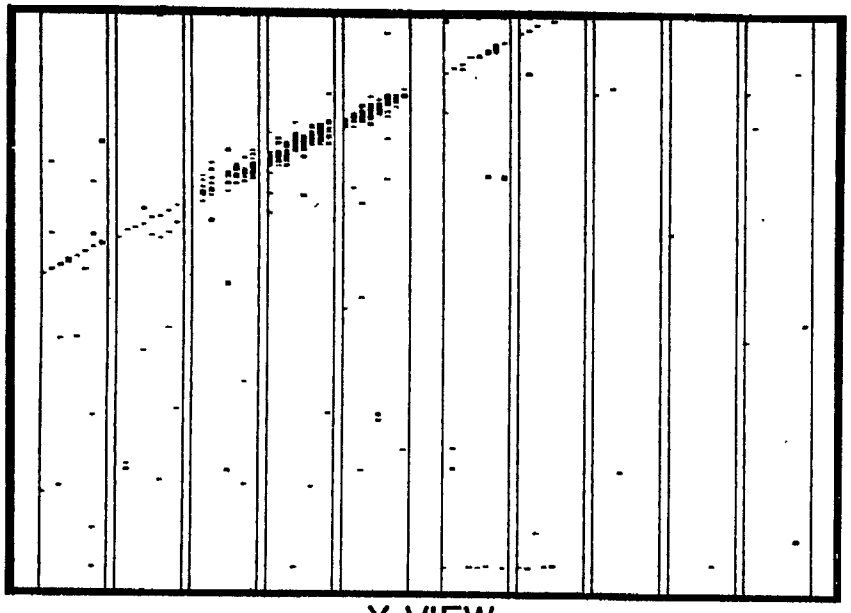

X VIEW

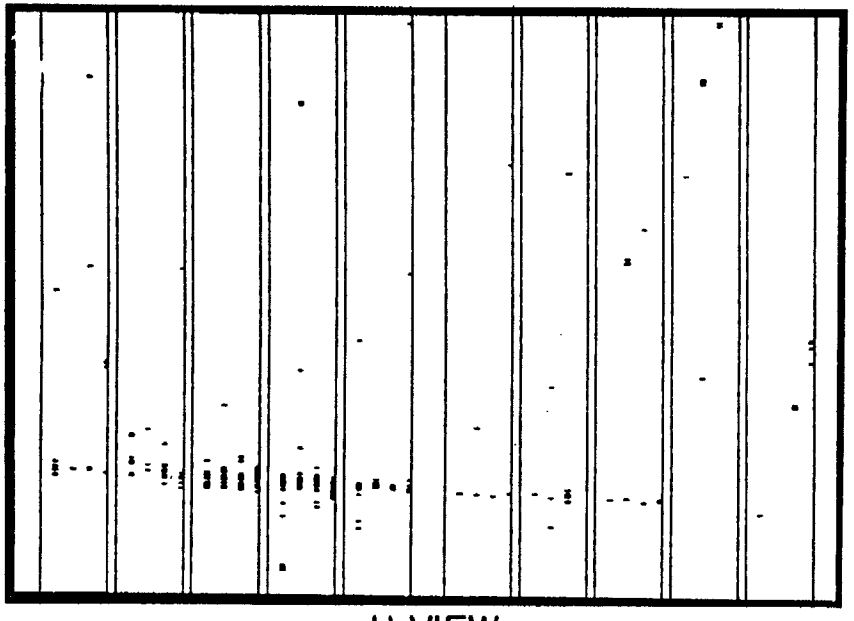

U VIEW

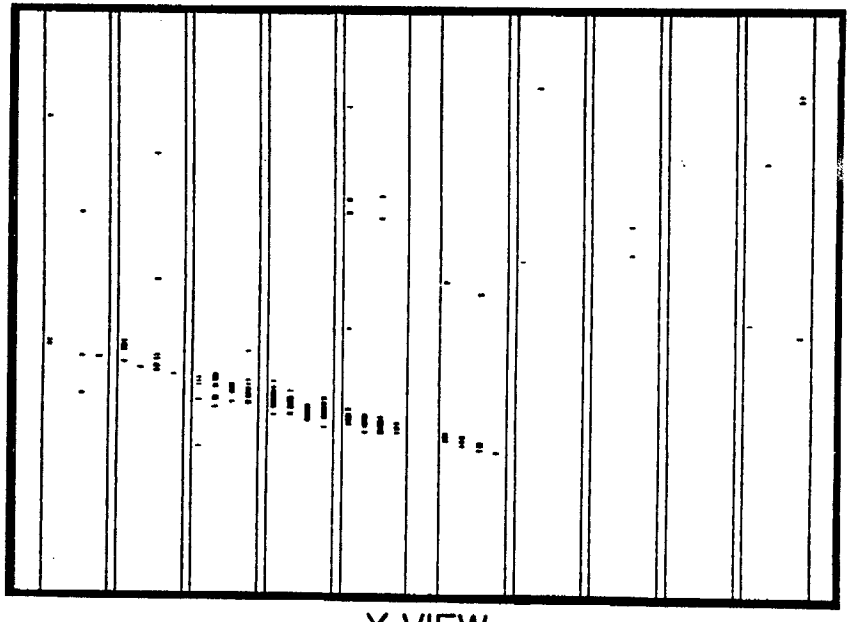

Y VIEW

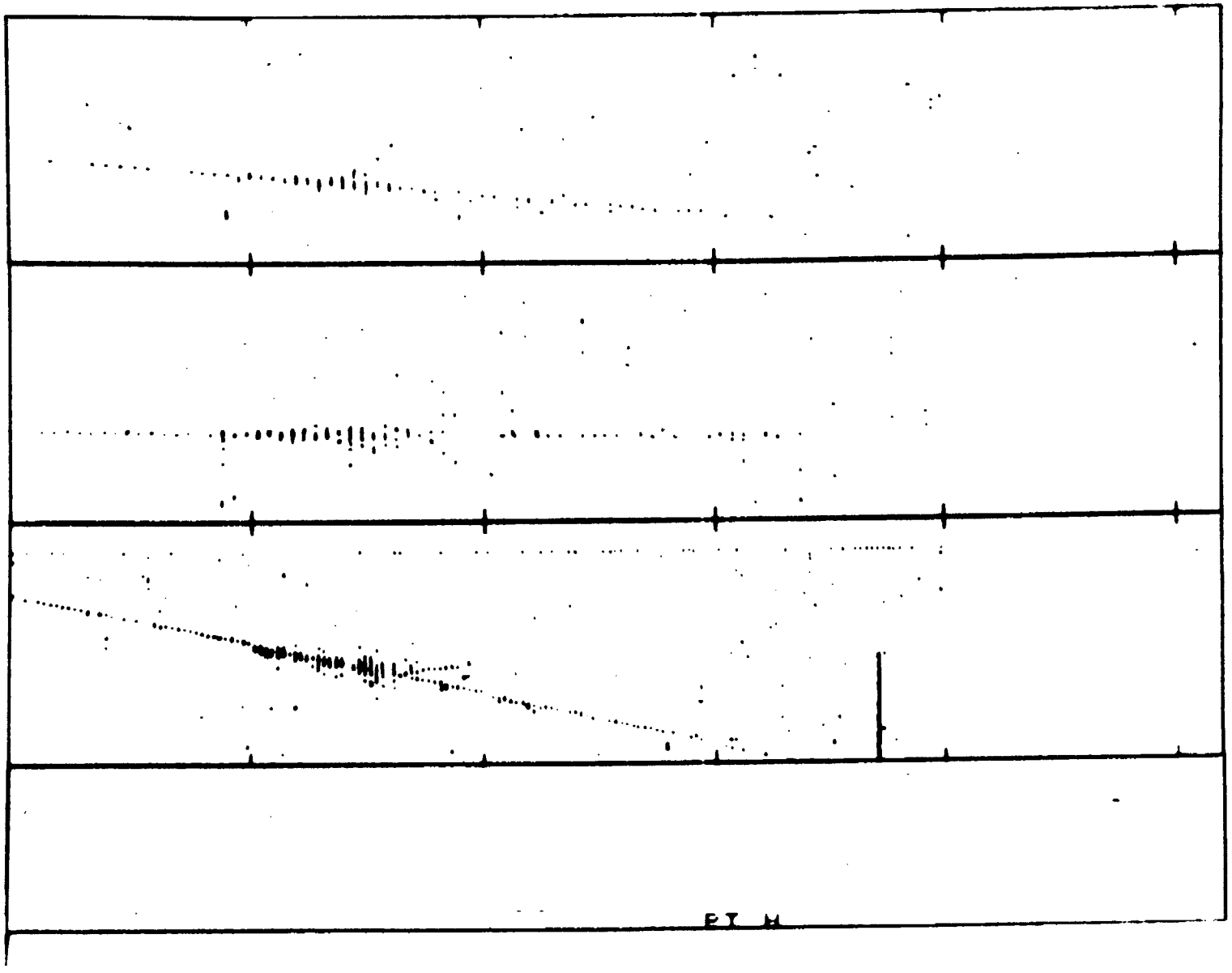
U
Y
X
PI M

APPENDIX B: BEAM SPILL STRATEGY

The protons should be spilled on the beam dump in a time structure which optimizes the number of neutrino interactions collected by the detector. There are three salient points to consider:

1. The Lab C detector has at present a dead time of approximately one second after triggering, leading to a loss of efficiency if the time between neutrino interactions is too small. This dead time may be reduced by a factor of ten using the appropriate gas mixture, however, we have not yet done the necessary tests to demonstrate this.
2. Triggers on cosmic rays are reduced to an acceptable level by requiring a minimum energy deposition in the detector; detailed studies using our detector are just beginning to investigate the minimum energy deposition which will be acceptable. Our aim is to get down to the level of about 1 GeV.
3. The probability that a high-energy muon traversing the detector interacts and deposits $\gtrsim$1 GeV is $\gtrsim 10^{-2}$; hence it will be necessary to detect and veto on the muon background. A dead time of $\sim$ 1 microsecond per entering muon will suffice to eliminate spurious triggers from this source.

For a spill of 10^{13} protons we expect an average of 3.3 neutrino interactions in the detector. In order to achieve a high efficiency for collecting these events it will be desirable to split the spill into a series of "pings" separated by one second. Figure B.1 shows the fraction of neutrino interactions which are logged as a function of the number of pings, assuming ping durations of one millisecond and negligible muon background. The optimal ping duration will balance the dead time due to muons with the false trigger rate due to cosmics. Figure B.2 shows the fraction of neutrino interactions which are logged as a function of the muon background for ping durations from one to one hundred milliseconds, assuming ten pings per spill. We will be able to achieve an efficiency of better than 75% while withstanding a background of up to 10^5 muons per spill of 10^{13} protons.

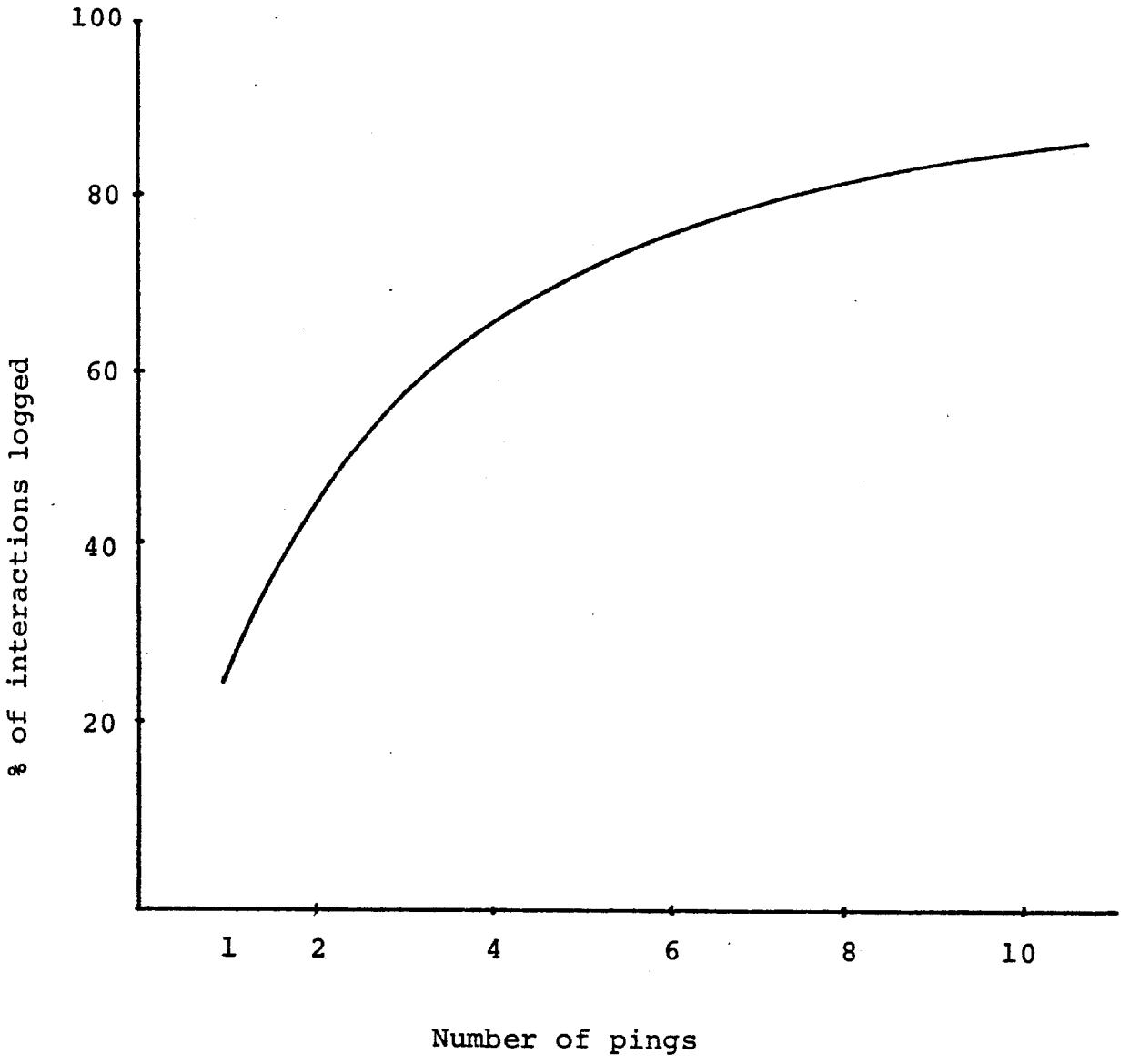
100
80
60
40
20
% of interactions logged
1
2
4
6
8
10
Number of pings

Figure B.1

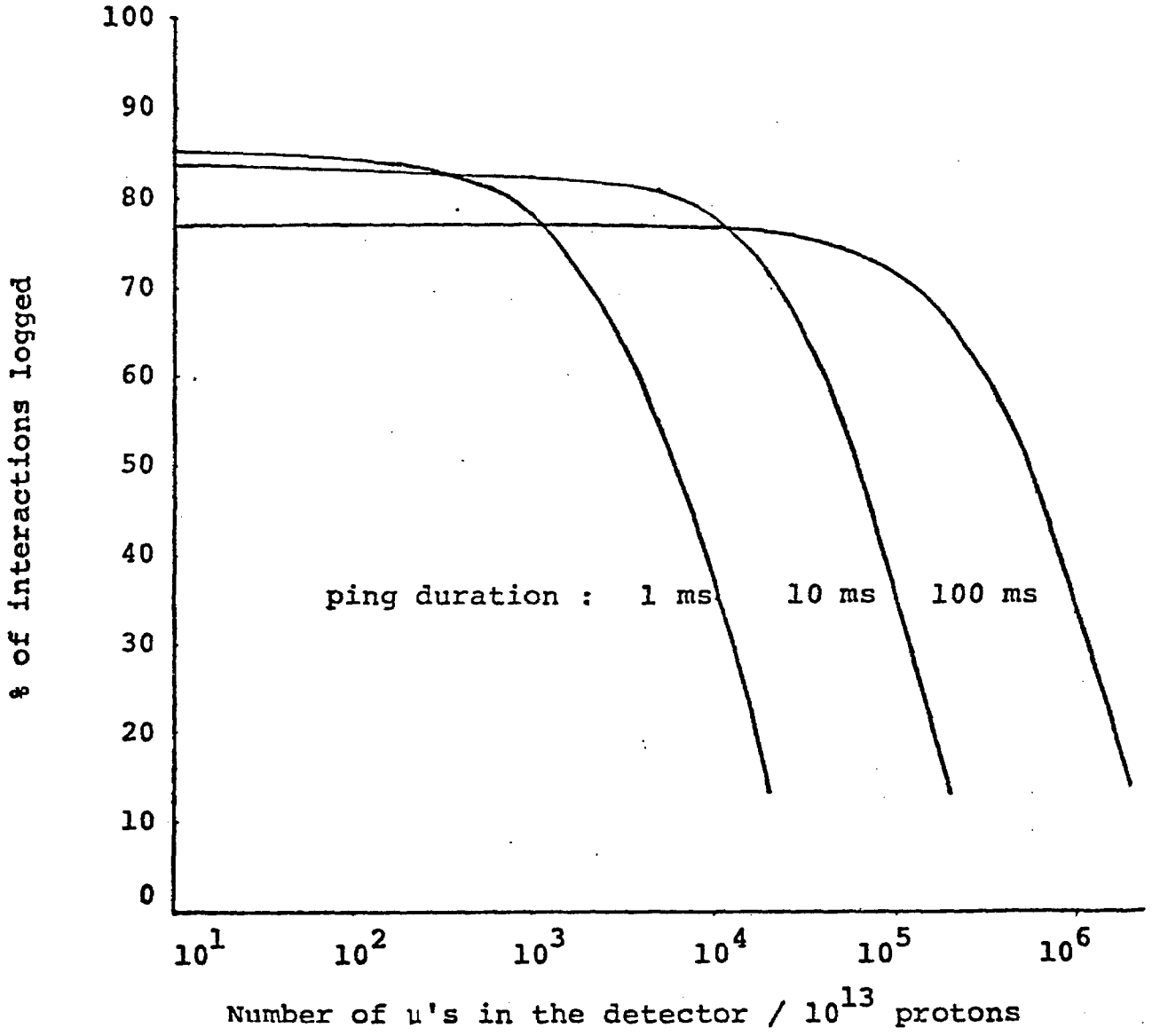
100
90
80
70
60
50
40
30
20
10
0
% of interactions logged
ping duration : 1 ms
10 ms
100 ms
10^1
10^2
10^3
10^4
10^5
10^6
Number of μ's in the detector / 10^{13} protons

Figure B.2

APPENDIX C:

In the proposal we have assumed that 1 TeV protonsare available concurrently with the development of a beam dump facility. There is also the possibility that the Tevatron will not be ready at that time. We wish to point out that a dump experiment will still be an exciting and viable project using 400 GeV protons.

For an equal number of protons on target, the fluxes of ν_e and ν_τ's will be down by about a factor of two at 400 GeV compared to the fluxes at 1 TeV. The average energy and thus the neutrino cross sections will be down by 2 1/2 so the yield of ν_τ events and ν_e elastic scatterings will be lower by a factor of 5. Likewise the primary backgrounds for these processes will be down by a factor of 5. The difference in cycle time between the two machines makes it feasable to request 10^{19} protons on target if 400 GeV protons are used. Thus the event rates would be similar.

At the lower energy we would use a cut of missing transverse momentum > 1 GeV in the $\tau \rightarrow \mu\nu\nu$ search. We would again have 50% of the τ decays in this channel survive this cut. Likewise the backgrounds for P_t > 1 GeV would scale with P . The important $\Delta\phi$ resolution is a weak function of energy. Both of these effects are due to the fact that the angular resolution degrades at low energy like 1/E, but that angles are larger by the same factor 1/E.

We believe that the physics objectives of running a beam dump in Lab C are topical and timely. Therefore funding for development and construction of such a beam dump facility should be provided as soon as possible. We anticipate that upon completion of the beam, we would like to run either 400 GeV or 1000 GeV protons, whichever are available.